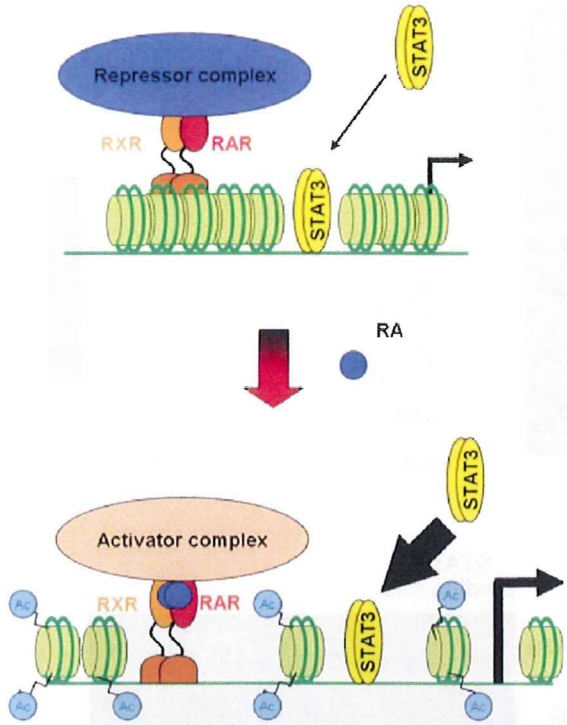

Figure 6. A model for synergistic activation of the *gfap* promoter by retinoic acid (RA) and leukemia inhibitory factor (LIF). In the absence of RA, RAR/RXR complexes with transcriptional repressors, leading to a closed chromatin structure. Upon ligand (RA) binding, the repressor complex is replaced by an activator complex, inducing a relaxed chromatin structure through histone H3 acetylation. This acetylation facilitates LIF-induced binding of STAT to its cognate sequence (see text for details). Abbreviation: Ac, acetyl group.

that either deleting this region or introducing nucleotide substitutions into the RARE augmented its responsiveness in NPCs treated with LIF alone. This is probably due to the impairment of binding of RAR/RXR, which can recruit a transcriptional repressor complex in the absence of ligand to the promoter [20–23]. It has been shown that ligand-free RAR/RXR heterodimers associate with corepressor molecules, such as N-CoR and SMRT (supporting information Fig. 4) [20–24]. A recent study indicated that astrocyte differentiation of NPCs was precociously and robustly enhanced in N-CoR-deficient embryonic forebrain, and that N-CoR-deficient NPCs did not self-renew but instead differentiated into astrocytes in vitro [18]. Moreover, overexpression of N-CoR in NPCs inhibited CNTF-mediated astrocytic differentiation. Collectively, these findings suggested that repressor complexes comprising ligand-free RAR/RXR and N-CoR are involved in the regulation of astrocyte-specific gene expression in NPCs.

It has been reported that RARα interacts with the src homology two (SH2) domain of STAT3 and that RAR/RXR associates with coactivator complexes including p300/CBP upon ligand binding [51]. In addition, STAT3 itself has been shown to associate with p300/CBP [13, 14]. It may therefore be possible that a large activator complex that includes RAR/RXR and STAT3 assembles on the *gfap* promoter in NPCs in response to combined treatment with RA and LIF. However, further experiments need to be conducted to assess this possibility.

Although gene knockouts of RAR and RA-synthesizing and -degrading enzymes, as well as the absence of retinoid in vitamin A-deficient mice, lead to defects in brain development such as abnormal positioning of the anterior and dorsal boundaries [27, 30, 34–38], the fate specification of embryonic NPCs in these mice has yet to be specifically addressed. Since we have shown here that RA promotes astrocyte differentiation of NPCs in collaboration with LIF, it will be intriguing to examine spatiotemporally regulated astrocyte differentiation of NPCs in such RA signal-dysregulated mice.

In conclusion, astrocyte differentiation of NPCs in the developing brain seems to be regulated by the intricate coordination of 1) the JAK-STAT pathway, which involves cross-talk with other signaling pathways at various steps such as regulation of STAT activation by LIF [7–9], 2) complex formation with other transcription factors [13], and 3) DNA [4] and histone modifications [50, 52, and this study].

Acknowledgments

We thank Dr. Y. Bessho and Dr. T. Matsui for valuable discussions; Dr. I. Smith and B. Juliandi for helpful comments and critical reading of the manuscript; N. Ueda and M. Tano for excellent secretarial assistance; and N. Namihira for technical help. This work was supported by the Brain Science Foundation, a Grant-in-Aid for Young Scientists, a Grant-in-Aid for Scientific Research on Priority Areas–Molecular Brain Science, and the Nara Institute of Science and Technology (NAIST) Global Center of Excellence (COE) Program from the Ministry of Education, Culture, Sports, Science and Technology of Japan.

Disclosure of Potential Conflicts of Interest

The authors indicate no potential conflicts of interest.

References

1 Qian X, Shen Q, Goderie SK et al. Timing of CNS cell generation: a programmed sequence of neuron and glial cell production from isolated murine cortical stem cells. Neuron 2000;28:69–80.
2 Sauvageot CM, Stiles CD. Molecular mechanisms controlling cortical gliogenesis. Curr Opin Neurobiol 2002;12:355–249.
3 Miller FD, Gauthier AS. Timing is everything: making neurons versus glia in the developing cortex. Neuron 2007;54:357–369.
4 Takizawa T, Nakashima K, Namihira M et al. DNA methylation is a critical cell-intrinsic determinant of astrocyte differentiation in the fetal brain. Dev Cell 2001;1:749–758.
5 Hsieh J, Gage FH. Epigenetic control of neural stem cell fate. Curr Opin Genet Dev 2004;14:461–469.
6 Namihira M, Kohyama J, Abematsu M et al. Epigenetic mechanisms regulating fate specification of neural stem cells. Philos Trans R Soc Lond B Bio Sci 2008;363:2099–2109.
7 Bonni A, Sun Y, Nadal-Vicens M et al. Regulation of gliogenesis in the central nervous system by the JAK-STAT signaling pathway. Science 1997;278:477–483.
8 Nakashima K, Wiese S, Yanagisawa M et al. Developmental requirement of gp130 signaling in neuronal survival and astrocyte differentiation. J Neurosci 1999;19:5429–5434.
9 Nakashima K, Taga T,Mechanisms underlying cytokine-mediated cell-fate regulation in the nervous system. Mol Neurobiol 2002;25: 233–244.

10 Bugga L, Gadient RA, Kwan K et al. Analysis of neuronal and glial phenotypes in brains of mice deficient in leukemia inhibitory factor. J Neurobiol 1998;36:509–524.
11 Koblar SA, Turnley AM, Classon BJ et al. Neural precursor differentiation into astrocytes requires signaling through the leukemia inhibitory factor receptor. Proc Natl Acad Sci U S A 1998;95:3178–3181.
12 He F, Ge W, Martinowich K et al. A positive autoregulatory loop of Jak-STAT signaling controls the onset of astrogliogenesis. Nat Neurosci 2005;8:616–625.
13 Nakashima K, Yanagisawa M, Arakawa H et al. Synergistic signaling in fetal brain by STAT3-Smad1 complex bridged by p300. Science 1999;284:479–482.
14 Sun Y, Nadal-Vicens M, Misono S et al. Neurogenin promotes neurogenesis and inhibits glial differentiation by independent mechanisms. Cell 2001;104:365–376.
15 Jaenisch R, Bird A. Epigenetic regulation of gene expression: how the genome integrates intrinsic and environmental signals. Nat Genet 2003;33:245–254.
16 Li B, Carey M, Workman JL. The role of chromatin during transcription. Cell 2007;128:707–719.
17 Fan G, Martinowich K, Chin MH et al. DNA methylation controls the timing of astrogliogenesis through regulation of JAK-STAT signaling. Development 2005;132:3345–3356.
18 Hermanson O, Jepsen K, Rosenfeld MG. N-CoR controls differentiation of neural stem cells into astrocytes. Nature 2002;419:934–939.
19 Ballas N, Mandel G. The many faces of REST oversee epigenetic programming of neuronal genes. Curr Opin Neurobiol 2005;15:500–506.
20 Freedman LP. Increasing the complexity of coactivation in nuclear receptor signaling. Cell 1999;97:5–8.
21 Aranda A, Pascual A. Nuclear hormone receptors and gene expression. Physiol Rev 2001;81:1269–1304.
22 Gronemeyer H, Gustafsson JA, Laudet V. Principles for modulation of the nuclear receptor superfamily. Nat Rev Drug Discov 2004;3:950–964.
23 Bastien J, Rochette-Egly C. Nuclear retinoid receptors and the transcription of retinoid-target genes. Gene 2004;328:1–16.
24 Jepsen K, Solum D, Zhou T et al. SMRT-mediated repression of an H3K27 demethylase in progression from neural stem cell to neuron. Nature 2007;450:415–420.
25 Epping ME, Wang L, Plumb JA et al. A functional genetic screen identities retinoic acid signalling as a target of histone deacetylase inhibitors. Proc Natl Acad Sci U S A 2007;104:17777–17782.
26 Mollard R, Viville S, Ward SJ et al. Tissue-specific expression of retinoic acid receptor isoform transcripts in the mouse embryo. Mech Dev 2000;94:223–232.
27 Sakai Y, Meno C, Fujii H et al. The retinoic acid-inactivating enzyme CYP26 is essential for establishing an uneven distribution of retinoic acid along the anterio-posterior axis within the mouse embryo. Genes Dev 2001;15:213–225.
28 Niederreither K, McCaffery P, Drager UC et al. Restricted expression and retinoic acid-induced downregulation of the retinaldehyde dehydrogenase type 2 (RALDH-2) gene during mouse development. Mech Dev 1997;62:67–78.
29 Koide T, Downes M, Chandraratna RA et al. Active repression of RAR signaling is required for head formation. Genes Dev 2001;15:2111–2121.
30 Sirbu IO, Gresh L, Barra J et al. Shifting boundaries of retinoic acid activity control hindbrain segmental gene expression. Development 2005;132:2611–2622.
31 Rawson NE, LaMantia AS. A speculative essay on retinoic acid regulation of neural stem cells in the developing and aging olfactory system. Exp Gerontol 2007;42:46–53.
32 Rossant J, Zirngibl R, Cado D et al. Expression of a retinoic acid response element-hsplacZ transgene defines specific domains of transcriptional activity during mouse embryogenesis. Genes Dev 1991;5:1333–1344.
33 Haskell GT, Lamantia AS. Retinoic acid signaling identifies a distinct precursor population in the developing and adult forebrain. J Neurosci 2005;25:7636–7647.
34 Halilagic A, Ribes V, Ghyselinck NB et al. Retinoids control anterior and dorsal properties in the developing forebrain. Dev Biol 2007;303:362–375.
35 Dupé V, Ghyselinck NB, Wendling O et al. Key roles of retinoic acid receptors alpha and beta in the patterning of the caudal hindbrain, pharyngeal arches and otocyst in the mouse. Development 1999;126:5051–5059.
36 Wendling O, Ghyselinck NB, Chambon P et al. Roles of retinoic acid receptors in early embryonic morphogenesis and hindbrain patterning. Development 2001;128:2031–2038.
37 Ribes V, Wang Z, Dollé P et al. Retinaldehyde dehydrogenase 2 (RALDH2)-mediated retinoic acid synthesis regulates early mouse embryonic forebrain development by controlling FGF and sonic hedgehog signaling. Development 2006;133:351–361.
38 White JC, Shankar VN, Highland M et al. Defects in embryonic hindbrain development and fetal resorption resulting from vitamin A deficiency in the rat are prevented by feeding pharmacological levels of all-*trans*-retinoic acid. Proc Natl Acad Sci U S A 1998;95:13459–13464.
39 Takahashi J, Palmer TD, Gage FH. Retinoic Acid and Neurotrophins collaborate to regulate neurogenesis in adult-derived neural stem cell cultures. J Neurobiol 1999;38:65–81.
40 Burette A, Jalenques I, Romand R. Developmental distribution of astrocytic proteins in the rat cochlear nucleus. Brain Res Dev Brain Res 1998;107:179–189.
41 Xu L, Glass CK, Rosenfeld MG. Coactivator and corepressor complex in nuclear receptor function. Curr Opin Genet Dev 1999;9:140–147.
42 Perissi V, Staszewski LM, McInerney EM et al. Molecular determinants of nuclear receptor-corepressor interaction. Genes Dev 1999;13:3198–3208.
43 Parnavelas JG. Glial cell lineages in the rat cerebral cortex. Exp Neurol 1999;156:418–429.
44 Ghaffari M, Whitsett JA, Yan C. Inhibition of hSP-B promoter in respiratory epithelial cells by a dominant negative retinoic acid receptor. Am J Physiol 1999;276:L398–404.
45 Bjorklund S, Almouzni G, Davidson I et al. Global transcription regulators of eukaryotes. Cell 1999;96:759–767.
46 Namihira M, Kohyama J, Semi K et al. Committed neuronal precursors confer astrocytic potential on residual neural precursor cells. Dev Cell 2009;16:245–255.
47 Sanosaka T, Namihira M, Nakashima K. Epigenetic mechanisms in sequential differentiation of neural stem cells. Epigenetics 2009;4:89–92.
48 Gottlicher M, Minucci S, Zhu P et al. Valproic acid defines a novel class of HDAC inhibitors inducing differentiation of transformed cells. EMBO J 2001;20:6969–6978.
49 Faigle R, Liu L, Cundiff P et al. Opposing effects of retinoid signaling on astrogliogenesis in embryonic day 13 and 17 cortical progenitor cells. J Neurochem 2008;106:1681–1698.
50 Donnell AO, Yang SH, Sharrocks AD. MAP kinase-mediated c-fos regulation relies on a histone acetylation relay switch. Mol Cell 2008;29:780–785.
51 Yang L, Lian X, Cowen A et al. Synergy between signal transducer and activator of transcription 3 and retinoic acid receptor-α in regulation of the surfactant protein B gene in the lung. Mol Endocrinol 2004;18:1520–1532.
52 Song MR, Ghosh A. FGF2-induced chromatin remodeling regulates CNTF-mediated gene expression and astrocyte differentiation. Nat Neurosci 2004;7:229–235.

nature neuroscience

ARTICLES

Wnt-mediated activation of NeuroD1 and retro-elements during adult neurogenesis

Tomoko Kuwabara[1], Jenny Hsieh[2,9], Alysson Muotri[3,9], Gene Yeo[4], Masaki Warashina[1,8], Dieter Chichung Lie[5], Lynne Moore[6], Kinichi Nakashima[7], Makoto Asashima[1] & Fred H Gage[6]

In adult hippocampus, new neurons are continuously generated from neural stem cells (NSCs), but the molecular mechanisms regulating adult neurogenesis remain elusive. We found that Wnt signaling, together with the removal of Sox2, triggered the expression of NeuroD1 in mice. This transcriptional regulatory mechanism was dependent on a DNA element containing overlapping Sox2 and T-cell factor/lymphoid enhancer factor (TCF/LEF)-binding sites (Sox/LEF) in the promoter. Notably, Sox/LEF sites were also found in long interspersed nuclear element 1 (LINE-1) elements, consistent with their critical roles in the transition of NSCs to proliferating neuronal progenitors. Our results describe a previously unknown Wnt-mediated regulatory mechanism that simultaneously coordinates activation of NeuroD1 and LINE-1, which is important for adult neurogenesis and survival of neuronal progenitors. Moreover, the discovery that LINE-1 retro-elements embedded in the mammalian genome can function as bi-directional promoters suggests that Sox/LEF regulatory sites may represent a general mechanism, at least in part, for relaying environmental signals to other nearby loci to promote adult hippocampal neurogenesis.

In the neurogenic niche of the adult mammalian brain, self-renewing NSCs give rise to committed neuronal progenitors in the subgranular zone (SGZ) of the dentate gyrus[1]. Astrocytes are an essential cell population that defines the SGZ niche and astrocyte-derived factors have instructive effects to promote adult neurogenesis[2,3]. Recently, it has been shown that Wnt3 expression persists in the adult hippocampus and Wnt3 is released by astrocytes to regulate adult neurogenesis *in vitro* and *in vivo*[4]. In the canonical Wnt/β-catenin pathway, the TCF transcription factor transduces Wnt/β-catenin signals to activate downstream target genes[4–9]. However, the target genes of Wnt/β-catenin signaling that are responsible for promoting adult neurogenesis have not been identified. Moreover, the regulatory mechanism underlying Wnt-mediated neuronal differentiation has not yet been elucidated.

NeuroD1 is a proneural basic helix-loop-helix (bHLH) transcription factor that is essential for the development of the CNS, particularly for the generation of granule cells in the hippocampus and cerebellum[10,11]. Environmental signals regulate adult neurogenesis, at least in part, through the activation of NeuroD1 (refs. 12,13). Previously, we found that overexpression of NeuroD is sufficient to promote neuronal differentiation in adult hippocampal neural progenitors[14], whereas deletion of NeuroD results in decreased survival and maturation of newborn neurons[15]. Thus, we hypothesized that astrocyte-derived Wnt signals may directly or indirectly regulate the transcription of NeuroD1 to control the transition of NSCs to committed neuronal progenitors.

The HMG-box transcription factor Sox2 is expressed in embryonic stem cells and most uncommitted cells in the developing CNS[16–18]. Sox2, which can be detected in cells of the mouse blastocyst, maintains precursor cells in a multipotent state[19–21]. During CNS development, Sox2 prevents neurogenesis[22] and forced expression of Sox2 results in the loss of proneural cells[23]. Overexpression of Sox2 in neural progenitor cells derived from embryonic ventricular zone permitted the differentiation of progenitors into astroglia, but it inhibited neurogenesis[24]. Although these analyses indicate that Sox2 is a transcriptional repressor of neuronal target genes during development, the exact nature of Sox2 regulation during adult neurogenesis remains elusive.

Here, we found that the transcriptional activation of NeuroD1 is dependent on canonical Wnt/β-catenin activation and removal of Sox2 repression from the *Neurod1* promoter in a sequence-specific manner. We discovered a previously unknown overlapping DNA-binding site corresponding to Sox2 and TCF/LEF (Sox/LEF) in the *Neurod1* promoter. Using retrovirus gene delivery of Sox2–Cre-GFP (Cre-GFP fusion protein under the control of the *Sox2* promoter, referred to here as $Sox2^{CRE}GFP$) into β-catenin conditional knockout (cKO) mice,

[1]National Institute of Advanced Industrial Science and Technology (AIST), Tsukuba Science City, Japan. [2]Department of Molecular Biology, Cecil H. and Ida Green Center for Reproductive Biology Sciences, University of Texas Southwestern Medical Center, Dallas, Texas, USA. [3]Department Pediatrics/Cellular & Molecular Medicine, School of Medicine, University of California San Diego, University of California San Diego Stem Cell Program, La Jolla, California, USA. [4]Cellular & Molecular Medicine, School of Medicine, University of California San Diego, La Jolla, California, USA. [5]Adult Neurogenesis and Neural Stem Cell Group, Institute of Developmental Genetics, Helmholtz Zentrum München, German Research Center for Environmental Health, Munich-Neuherberg, Germany. [6]Laboratory of Genetics, The Salk Institute, La Jolla, California, USA. [7]Laboratory of Molecular Neuroscience, Graduate School of Biological Sciences, Nara Institute of Science and Technology, Ikoma, Japan. [8]Present address: Cell Biology Research Center, Genome Research Laboratories, Wako Pure Chemical Industries, Ltd., Amagasaki, Hyogo, Japan. [9]These authors contributed equally to this work. Correspondence should be addressed to T.K. (t.warashina@aist.go.jp).

Received 12 March; accepted 22 May; published online 23 August 2009; doi:10.1038/nn.2360

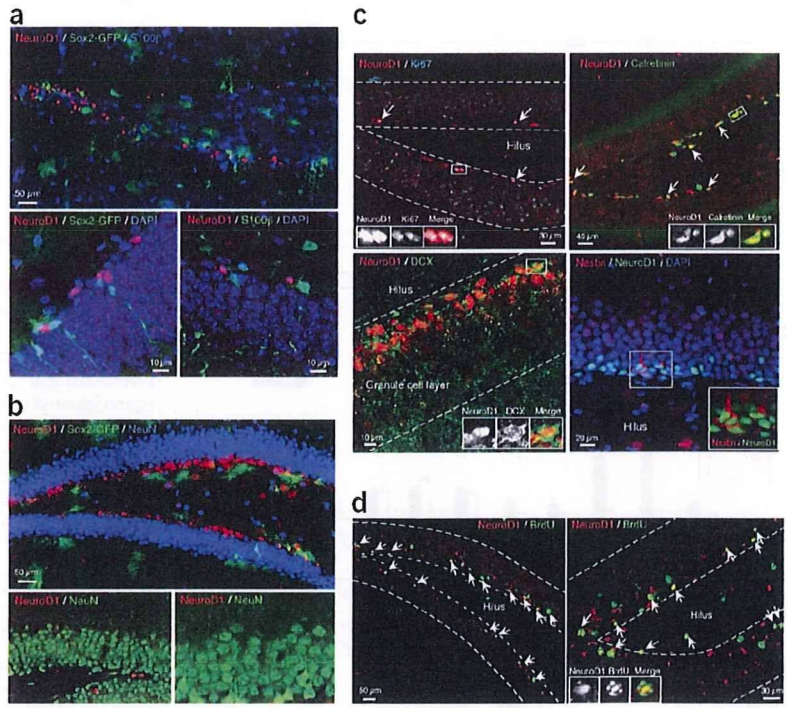

Figure 1 Specific expression of the *Neurod1* gene in early committed neurogenic cells in adult hippocampus. (**a**) Immunohistochemical analysis of neurogenic dentate gyrus area in adult hippocampus of the transgenic mouse that has a *Sox2* promoter–driven EGFP reporter. Top, Sox2 is shown in green, and we stained for NeuroD1 (red) and S100β (blue). Bottom left, a higher-magnification image is shown with DAPI staining (blue) Bottom right, section stained for NeuroD1 (red), S100β (green) and DAPI (blue). (**b**) Distinct population of neuroblast cells expressing the *Neurod1* gene and mature neurons in adult mouse hippocampus. Top, Sox2 is shown in green in adult hippocampus of a *Sox2* promoter–driven EGFP reporter transgenic mouse; we also stained for NeuroD1 (red) and NeuN (blue). Bottom, NeuroD1-positive cells (red) and NeuN-positive cells (green) were exclusive to the inner layer of the dentate gyrus. (**c**) Immunocytochemical analysis of NeuroD1-positive cells in adult rat hippocampus. NeuroD1-positive cells (red) colocalized with Ki67 (cyan). White arrows indicate colocalizing cells; the region in the white square is magnified in a separate window. Bottom left, NeuroD1-positive cells (red) colocalized calretinin (green) and DCX (green). Bottom right, some NeuroD1-positive cells (green) colocalized with nestin (red). White arrows indicate populations of colocalized cells for both markers. (**d**) Proliferative status of NeuroD1-positive cells in adult hippocampus. BrdU (100 mg per kg of body weight) was injected for 1 week into Fisher 344 rats (7–8 weeks old). Cells that were double positive for NeuroD1 (red) and BrdU (green) are indicated by white arrows. The colocalizing cell (NeuroD1 and BrdU positive) in the white square is magnified on the right.

we observed a significant loss ($P < 0.001$; data represent mean ± s.d., $n = 6$ per group) of NeuroD1-positive progenitors as well as a decrease in newborn granule neurons, with no effect on the stem/progenitor cell pool. These findings are extended to the regulation of LINE-1 retrotransposon expression through silencing and activation of Sox2 and Wnt/β-catenin, respectively, which is consistent with LINE-1 being critical during neuronal differentiation[25]. Together, these results suggest that Wnt-mediated activation of NeuroD1 and LINE-1 is coordinately regulated during adult neurogenesis, which may extend to other nearby genomic loci using the bi-directionality of Sox/LEF sites. These findings also suggest that crosstalk between Sox2 and Wnt/β-catenin signaling represents an important mechanism underlying neuronal differentiation.

RESULTS

The expression of Sox2 and NeuroD1 in adult neurogenesis

To characterize the expression of transcription factors in adult dentate gyrus, we performed immunohistochemical analysis in the Sox2–enhanced GFP (EGFP) transgenic mouse[1,26]. NeuroD1-positive cells were clearly detected in the SGZ region of the dentate gyrus and did not colocalize with Sox2-GFP or S100β, a marker of astrocytes (**Fig. 1a**). Moreover, Sox2-positive and NeuroD1-positive cells were mutually exclusive with mature neurons, suggesting that Sox2 and NeuroD1 counteract one another to regulate the early stages of adult neurogenesis (**Fig. 1b**).

To further define the properties of NeuroD1-positive cells, we examined additional markers of stem/progenitor cells and immature granule neurons. NeuroD1-positive cells colocalized with nestin, calretinin and doublecortin (DCX; **Fig. 1c**). Sox2-GFP cells colocalized with the radial glial cell marker nestin, whereas only a few weakly stained GFP-positive cells colocalized with the weaker DCX-positive cells[1]. A majority of the NeuroD1-positive cells colocalized with DCX, whereas only a few cells were nestin positive, suggesting that NeuroD1-positive cells have recently transitioned from Sox2-positive NSCs to neuronal progenitors/immature neurons (**Fig. 1c**). In addition, NeuroD1-positive cells colocalized with Ki67 (**Fig. 1c**), indicating that they are among the proliferating population in adult dentate gyrus. To further examine their proliferative status, we treated Fischer 344 rats with BrdU and found that NeuroD1-positive cells colocalized with BrdU-positive cells in the SGZ (**Fig. 1d**). Taken together, these data indicate that NeuroD1 is transiently expressed in dividing progenitor cells and immature granule neurons in adult dentate gyrus and suggest that the expression of Sox2 and NeuroD1 must be coordinately regulated during adult neurogenesis.

Sox/LEF DNA recognition motif in the *Neurod1* promoter

Next, we surveyed 3 kb of the regulatory region upstream of the *Neurod1* and *Neurod2* promoters and found binding sites for the TCF/LEF and Sox transcription factors (**Fig. 2a**). Notably, some Sox and TCF/LEF sequences were found to overlap with each other, forming a previously unknown binding motif, which we refer to as the Sox/LEF-binding site, that was conserved among humans, rats and mice (**Fig. 2b**).

Using an established adult rat hippocampal NSC line[27], we compared the relative expression levels of *Sox2*, *Neurod1* and other pro-neural genes. Adult NSCs expressed high levels of Sox2 in undifferentiated stages (**Fig. 2c**), but Sox-2 expression was reduced in neurons. In contrast, both NeuroD1 and NeuroD2 were significantly upregulated ($P < 0.001$) in neurons (**Fig. 2c**). Notably, induction levels of NeuroD1 and NeuroD2 were higher than those of Neurog1 and Neurog2, which function as important bHLH proteins during neural development[28–30]. Gene activation by Wnt/β-catenin signaling requires

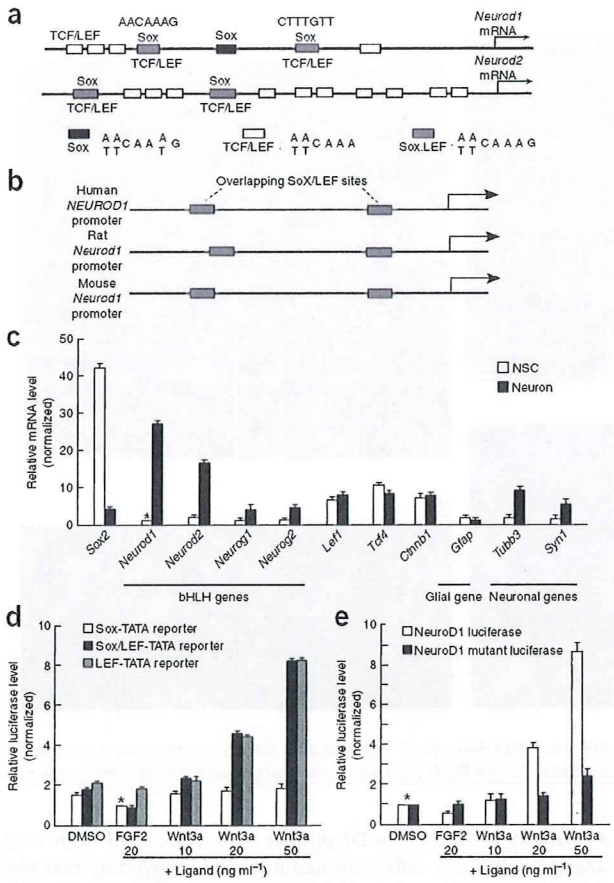

Figure 2 Sox2/LEF DNA regulatory elements on the *Neurod* promoters. (**a**) Schematic representation of the binding sites of TCF/LEF and Sox transcription factors on the 3-kb promoters of the *Neurod1* and *Neurod2* genes. The sequences of the DNA regulatory elements recognized by Sox2 (black box) and TCF/LEF (white box) and the overlapping DNA regulatory consensus sequence (Sox/LEF; gray box) recognized by both Sox2 and TCF/LEF are shown (bottom). (**b**) Schematic representation of the Sox2/LEF-binding sites (gray boxes) in human, rat, and mouse *Neurod1* promoters. (**c**) Comparison of expression levels between NSCs and differentiating neurons by quantitative real-time PCR (qRT-PCR) of genes related to Wnt signaling. The expression level of *Gfap* as a typical glial gene was assessed. Expression levels of β-tubulin III (*Tubb3*) and synapsin I (*Syn1*) were also analyzed as neuronal genes. Each mRNA value was normalized to that of *Gapdh* and then plotted as the fold increase of the sample of *Neurod1* mRNA in NSCs (asterisk). (**d**) Simple reporter assay with the regulatory elements of Sox2, TCF/LEF and Sox/LEF transcription factors. The luciferase value was normalized to a sample with a Sox-TATA reporter construct, with an FGF2 ligand (asterisk). (**e**) Activity of the *Neurod1* promoter. A 1.5-kb *Neurod1* promoter region (including a Sox/LEF site and a TCF/LEF site) was linked to the *luciferase* gene. The reporter construct with mutation at the Sox/LEF site on the *Neurod1* promoter (NeuroD1 mutant luciferase) was also introduced to the adult NSCs. Luciferase value was normalized to sample with DMSO as a control ligand (asterisk).

stabilization of the β-catenin protein and nuclear association with TCF/LEF[9]. We found that the mRNA levels of β-catenin, TCF and LEF1 remained unchanged during neuronal differentiation, suggesting that Wnt and β-catenin are regulated at the post-transcriptional level (**Fig. 2c**).

To investigate the requirement of the Sox/LEF sequence, we prepared a set of reporter constructs (Sox-, Sox/LEF- and LEF-TATA; Online Methods). Incubation with fibroblast growth factor 2 (FGF2), which maintains cells in an undifferentiated state, reduced luciferase activity resulting from the Sox-TATA and Sox/LEF-TATA constructs, but not from the LEF-TATA construct, compared with the luciferase activity in cells treated with DMSO. This finding suggests that the Sox regulatory element has a negative role on transcription in the presence of FGF2, whereas the LEF regulatory element itself has no effect. When the Wnt3a ligand was introduced to cells, we observed a clear dose-dependent upregulation of luciferase in cells expressing the Sox/LEF-TATA and LEF-TATA constructs (**Fig. 2d**). The Sox regulatory element itself had almost no effect in the presence of Wnt3a, indicating that there is an apparent functional difference in the Sox and LEF regulatory elements with regard to ligand response.

Next, we introduced the Wnt3a ligand into NSCs and observed a dose-dependent upregulation of *Neurod1* promoter activity (**Fig. 2e**). In contrast, when the mutant reporter construct (NeuroD1 mutant luciferase (**Fig. 2e**) contains a mutation in the Sox/LEF site to abolish Sox2 and TCF/LEF binding) was introduced into NSCs, we failed to observe either a reduction in luciferase activity in the undifferentiated state (FGF2 ligand) or an increase in luciferase activity by the addition of Wnt3a ligand (**Fig. 2e**). These data suggest that the Sox/LEF binding sequence in the *Neurod1* promoter is important for discriminating between both TCF/LEF- and Sox2-mediated transcriptional regulation during adult neurogenesis.

Upregulation of NeuroD1 is dependent on the Sox/LEF site

To investigate the regulatory mechanism underlying *Neurod1* gene transcription, we compared the expression of NeuroD1 with that of proteins in the Wnt signaling pathway. S100β-positive and glial fibrillary acidic protein (GFAP)-positive astrocytes were also positive for both Wnt3 and Wnt3a, consistent with published results[4] (**Supplementary Fig. 1**). Following neuronal differentiation *in vitro*, NeuroD1 expression peaked at 1 d after neuronal induction and diminished by 4 d. In protein blotting experiments, we found that Sox2 was expressed in undifferentiated NSCs and downregulated on neuronal differentiation (**Fig. 3a**). In contrast, β-catenin was clearly stabilized and accumulated when NeuroD1 was highly expressed, although the level of β-catenin mRNA was unchanged (**Fig. 2c**). These results suggest that NeuroD1 expression is temporally regulated, consistent with NeuroD1 expression *in vivo*, and Wnt/β-catenin activation and de-silencing of Sox2 may be involved in promoting neuronal differentiation.

For Wnt-mediated transcriptional activation of target genes, the phosphorylated, inactive form of GSK3β is the canonical enhancer for the stabilization of β-catenin protein[9]. Thus, we assessed whether neuronal differentiation in adult NSCs influenced the phosphorylation of GSK3β. As hypothesized, GSK3β phosphorylation was triggered on neuronal differentiation, whereas total GSK3β levels remained unchanged (**Fig. 3b**).

To evaluate the effects of Wnt signaling on *Neurod1* gene activity, we carried out gain-of-function studies using Wnt3a-expressing lentivirus[4] and a pharmacological inhibitor of GSK3β (TDZD8). For loss-of-function studies, we used a full-length cDNA *Sox2* construct, a secreted mutant Wnt (dominant-negative Wnt, DnWnt) construct[4], a small hairpin RNA (shRNA) that was specific to β-catenin mRNA (**Supplementary Fig. 2**) and the Wnt antagonist Dickkopf1 (Dkk1). *Neurod1* mRNA levels were strongly increased by both Wnt3a expression and the GSK3β inhibitor (**Fig. 3c**). In contrast, Dkk1, DnWnt and an shRNA to β-catenin reduced NeuroD1 expression. To further examine the effect of Wnt3a expression on NeuroD1 transcriptional activation, we introduced a NeuroD1 luciferase construct into adult

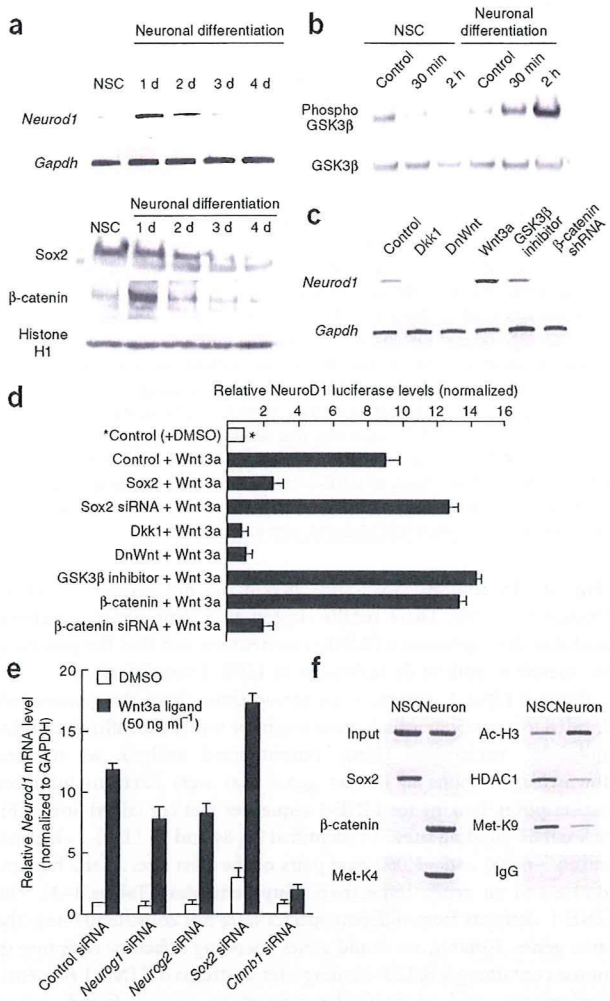

Figure 3 Wnt signaling increases *Neurod1* promoter activity during early neurogenesis. (**a**) Time course of *Neurod1* mRNA expression during the early stages of neurogenesis in cultured adult NSCs. RT-PCR detection of *Neurod1* and *Gapdh* is shown. Western blots of Sox2 and β-catenin during neurogenesis in cultured adult NSCs are shown in the lower panels. (**b**) Induction of a phosphorylated inactive form of GSK3β to stabilize β-catenin during Wnt signaling in early committed neurogenic cells. Western blots of both GSK3β and phosphorylated GSK3β were conducted using the same neuronal induction treatment. (**c**) The effect of Wnt signaling on the expression of *Neurod1* mRNA. RT-PCR analysis using total RNA extracted from adult NSCs treated with Dkk1, DnWnt, Wnt3, TDZD8 or β-catenin shRNA. (**d**) The effect of Wnt signaling on the promoter activity of the *Neurod1* gene. The luciferase value was normalized to that of cultured NSC sample with control vector and control ligand (DMSO, asterisk, white bar). (**e**) The effect of siRNAs targeting Neurog1, Neurog2, Sox2 and β-catenin on Wnt3a ligand–mediated induction on *Neurod1* mRNA. qRT-PCR analysis for *Neurod1* mRNA was plotted. The amount of mRNA present for each sample was normalized to that of *Gapdh* and then plotted as the fold increase over the control (control siRNA with DMSO). (**f**) ChIP analysis at the *Neurod1* promoter in adult neurogenesis. PCR primers were designed to surround the Sox/LEF sequence on the rat *Neurod1* promoter.

NSCs. Sox2, Dkk1 and DnWnt expression all had negative effects on Wnt3a-mediated NeuroD1 transcriptional activation. In contrast, *Neurod1* promoter activity was further enhanced by the constitutively active form of β-catenin and by TDZD8 (**Fig. 3d**).

To confirm that the transcriptional activation of NeuroD1 is dependent on the Wnt3a ligand, we introduced several sets of synthesized small interfering RNAs (siRNAs) into adult NSCs. Wnt3a ligand increased *Neurod1* mRNA expression (~12-fold increase) in control siRNA-transfected cells (**Fig. 3e**). In contrast, β-catenin siRNA substantially reduced NeuroD1 activation on Wnt3a ligand treatment (~sixfold decrease). Notably, we did not observe substantial reduction of Wnt3a-mediated NeuroD1 activation by Neurog1 and Neurog2 siRNAs, indicating that Wnt3a effects on NeuroD1 may be direct. The amount of NeuroD1 mRNA increased in cells treated with Sox2 siRNA more than in cells treated with control siRNA, possibly as a result of residual endogenous Sox2 protein at the onset of neuronal induction (**Fig. 3a**), which may have a negative influence on NeuroD1 expression.

Finally, we performed chromatin immunoprecipitation (ChIP) analysis to assess protein association. We found that Sox2 and the histone deacetylase HDAC1 repressor protein were associated on the endogenous *Neurod1* promoter, specifically at the Sox/LEF site, in undifferentiated NSCs, and that this association diminished when the neurons differentiated (**Fig. 3f**). Consistently, di-methylated histone H3 at Lys9 (K9), commonly associated with transcriptional repression[31], was also present in NSCs. Moreover, β-catenin, acetylated histone H3 and methylated histone H3 at Lys4 (K4), all of which are associated with transcriptional activation, were observed on the *Neurod1* promoter locus in neuronal cells, suggesting that *Neurod1* gene transcription is mediated by an active process. These results suggest that the conversion of a Sox2 repressor complex to a β-catenin activator complex is associated with chromatin remodeling on neuronal induction.

Wnt3a-dependent activation of LINE-1 retrotransposon

Sox2 can suppress LINE-1 expression in adult NSCs[25]. The observation that Sox2 is downregulated at nearly the same time that β-catenin is upregulated raises the possibility that they may target the same Sox/LEF regulatory sequences in neuronal genes. Indeed, many Sox/LEF-binding sites were present throughout the entire LINE-1 sequence, including several sites in open reading frame 2 (ORF2; **Fig. 4a**). We next determined whether these sequences were functional using reporter assays in adult NSCs.

We previously reported that promoter activity in the human LINE-1 5′ untranslated region (UTR) is increased during neuronal differentiation compared with undifferentiated cells[25]. We confirmed this observation using a reporter construct containing the LINE-1 5′ UTR in both forward and reverse orientation upstream of the *luciferase* gene (**Fig. 4b**). Because ORF2 of LINE-1 contains several Sox/LEF-binding sites, we cloned the LINE-1 ORF2 portion and linked it to the *luciferase* gene to assess putative promoter activity. The ORF2 sequence demonstrated promoter activity in both forward and reverse orientation during neuronal differentiation. The activity was highest 1 d after neuronal induction and it gradually declined during neuronal differentiation. This transient upregulation immediately after neuronal induction was common to both LINE-1 5′ UTR– and ORF2-based reporter constructs (**Fig. 4b**), a finding that is also consistent with the expression dynamics of NeuroD1 (**Fig. 3a**).

LINE-1 sequences comprise a substantial part of the genome, and because the Sox/LEF sites are clustered in LINE-1 sequences, they are also prevalent in the genome. Using ChIP, we found that Sox2 and HDAC were associated in undifferentiated NSCs in which LINE-1 was silenced (**Fig. 4c**), similar to their association on the *Neurod1* promoter (**Fig. 3f**). On the other hand, we observed that β-catenin and acetylated histone H3 associated with each other in neurons. To investigate Wnt3a

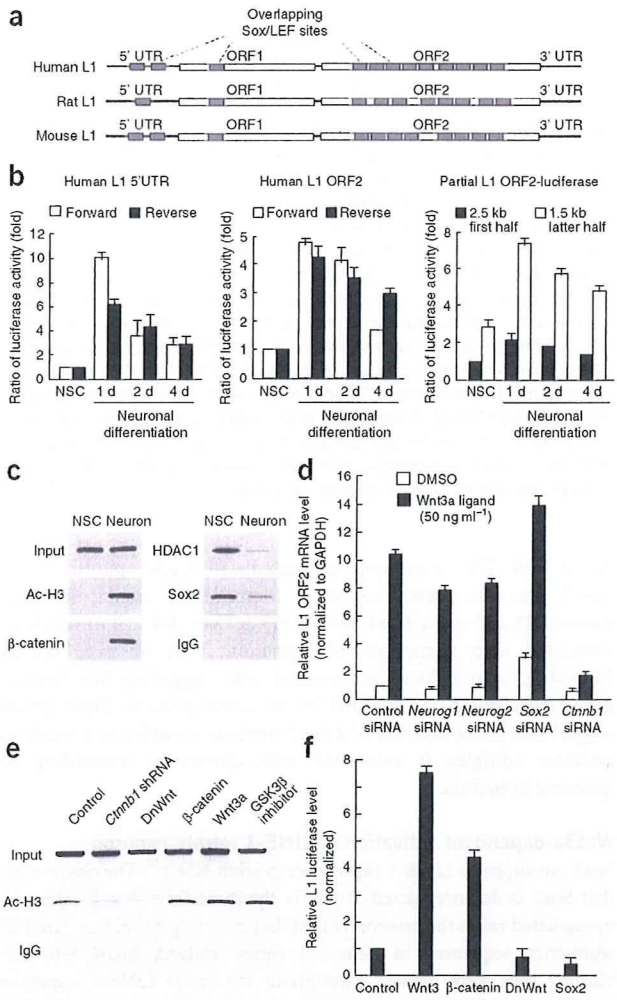

Figure 4 Effect of Wnt signaling on the expression of NeuroD1 and LINE-1 during adult neurogenesis. (**a**) DNA regulatory elements recognized by Sox2 and TCF/LEF transcription in LINE-1. A schematic representation of the Sox/LEF DNA regulatory elements (gray boxes) in the human, rat, and mouse retrotransposon LINE-1 is shown. (**b**) Promoter activity of the 5′ UTR and ORF fragment of LINE-1 during adult neurogenesis. Luciferase constructs with 5′ UTR and LINE-1 ORF2 sequences linked to the *luciferase* gene, in both forward (white) and reverse (black) orientations, were introduced into adult NSCs by lentivirus infection (left and middle panels). Partial fragments of the LINE-1 ORF2, the first 2.5 kb (black columns) and the last 1.5 kb (white columns), were also linked to the *luciferase* gene in the reporter assay (right). (**c**) ChIP analysis of rat LINE-1. PCR primers were designed to surround the Sox/LEF DNA regulatory elements. (**d**) Wnt3a-mediated induced production of LINE-1 ORF2 mRNA. The induction level was measured by qRT-PCR with several synthesized siRNAs. The mRNA level was normalized to that of *Gapdh* and then plotted as the fold increase over the control (control siRNA with DMSO). (**e**) The effect of Wnt signaling on the chromatin remodeling of LINE-1. Activation of the chromatin state (acetylation of histone H3) in the LINE-1 sequences was assessed using several Wnt-related constructs. (**f**) The activation and repression of the LINE-1 promoter. The effect of Wnt on the activity of LINE-1–based promoters was examined using the LINE-1 luciferase construct. After 1 d in the culture, luciferase assays were performed on adult NSCs treated with each construct.

ligand–mediated transcriptional activation of LINE-1 mRNAs, we compared the induction levels of LINE-1 in cells given control siRNA with the cells treated with several gene-specific siRNAs. Wnt3a ligand caused a tenfold increase in the amount of LINE-1 ORF2 mRNA in cells treated with control siRNA (**Fig. 4d**). When cells were treated with β-catenin siRNA, Wnt3a ligand–induced activation was almost abolished, whereas treatment with Neurog1 and Neurog2 siRNAs had almost no effect on Wnt3a-mediated stimulation. On introduction of Sox2 siRNA, endogenous LINE-1 was upregulated and Wnt3a-mediated stimulation of LINE-1 was increased (**Fig. 4d**).

Next, we examined the chromatin status (acetylated histone H3) in the LINE-1 element. β-catenin shRNA and DnWnt stopped the chromatin from switching from the silenced state to the activated state (**Fig. 4e**). The expression of endogenous LINE-1 mRNA was also downregulated by β-catenin shRNA (**Supplementary Fig. 2**), consistent with our ChIP data. The addition of Wnt3, β-catenin or TDZD8 increased acetylated histone H3 levels in the LINE-1 genomic region, indicating that Wnt signaling itself could induce the active chromatin state, directly or indirectly, in the LINE-1 locus (**Fig. 4e**).

We also examined the effect of Wnt3a on the activity of LINE-1–based promoters using the LINE-1 luciferase construct. β-catenin and Wnt3a enhanced LINE-1 luciferase activity significantly ($P < 0.001$) (**Fig. 4f**). In contrast, Sox2 and DnWnt did not promote LINE-1–promoter activity. These results suggest that Wnt signaling actively mediates the expression of LINE-1 in neurons and that the process is not merely a result of de-repression of LINE-1 transcription.

Because LINE-1 sequences are spread throughout the genome, we decided to investigate which genes might be under the influence of this molecular mechanism. Using computational analysis, we scanned downstream regions of human genes that were likely to influence transcription, looking for LINE-1 sequences that contained Sox2, LEF or Sox/LEF-binding sites. We identified 79, 84 and 25 LINE-1 elements within −6,000 and +1,000 base pairs of the start sites of the human, mouse and rat genes, respectively (**Supplementary Tables 1–3**). The LINE-1 elements from different species were not consistently near the same genes. Notably, we found genes encoding olfactory receptors in mouse containing Sox/LEF-binding sites upstream of LINE-1 elements. Furthermore, and of particular interest to us, we found several neuronally relevant genes that may be susceptible to the repressor/activator mechanism described above, including, for example, DCX and Neuregulin 4, or related to cell cycle (SCAPER (zinc finger protein 291) and mitogen-activated protein kinase 10; **Supplementary Tables 1–3**).

Role of β-catenin in neuronal differentiation of adult NSCs

We further investigated the effect of Wnt/β-catenin signaling on cell fate choice *in vivo*. A retrovirus encoding *Sox2* promoter–driven *cre-gfp* ($Sox2^{CRE}GFP$)[1] was injected into the dentate gyrus of $Ctnnb1^{loxP/loxP}$ mice (β-catenin cKO; **Supplementary Fig. 3**)[32]. Because a retrovirus only transduces one of the two daughter cells of dividing cells, single-cell clones are generated by the conversion of Sox2-positive cells to differentiated lineages in β-catenin cKO mice.

To identify the composition of cell types in the Sox2 lineage, we carried out an immunohistochemical analysis (**Figs. 5** and **6**). The number of total GFP-positive cells in β-catenin cKO mice was decreased by about 50% compared with control mice (**Fig. 5b**). In control mice, many $Sox2^{CRE}GFP$-positive cells colocalized with NeuroD1-positive cells (**Fig. 5a**). In contrast, the proportion of ND1 and GFP double-positive cells in β-catenin cKO mice was decreased by 92% relative to that of control mice (**Fig. 5c,d**). In addition to NeuroD1, $Sox2^{CRE}GFP$-positive cells that colocalized with markers for newborn neurons, such as DCX (**Supplementary Fig. 4**) and TUJ1 (**Supplementary Fig. 5**), were

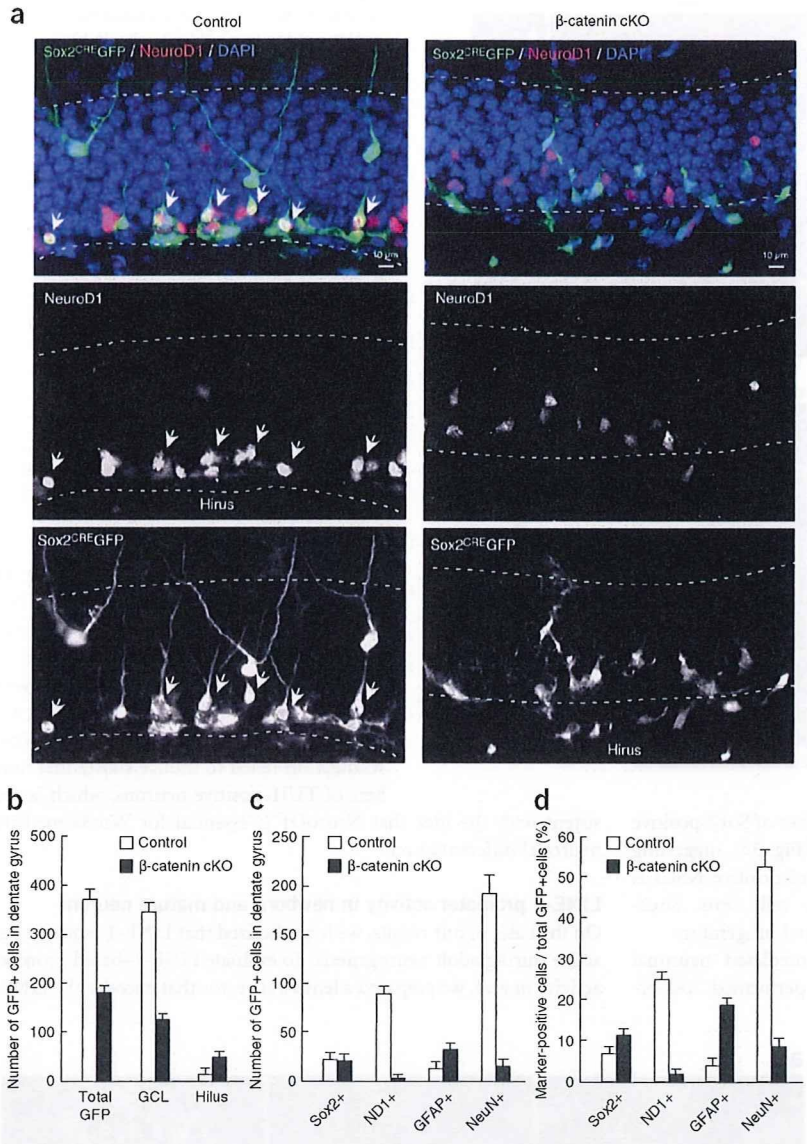

Figure 5 Adult NSC cannot transition to immature and mature granule neurons in β-catenin cKO mice. Immunohistochemical analysis of the Sox2^{CRE}GFP cells. (**a**) Sox2^{CRE}GFP retrovirus was injected into the dentate gyrus of control mice (left) or β-catenin cKO mice (right). Immunohistochemical analysis of NeuroD1 (red), GFP (green) and DAPI (blue) in both groups is shown and GFP-positive cells colocalized with NeuroD1-positive cells in control mice (indicated by white arrows, left panels). In control mice, GFP-positive cells were present among the more differentiated neurons deeper in the granule cell layer (left). In β-catenin cKO mice, GFP-positive cells were observed more often near or in the hilus region, rather than among the more differentiated neurons deeper in the granule cell layer. (**b**) Numbers of GFP-positive cells in the dentate gyrus of control mice (white bars) and β-catenin cKO mice (black bars). (**c**) Numbers of marker and GFP double-positive cells in the dentage gyrus of control mice (white bars) and β-catenin cKO mice (black bars). (**d**) Percentages of marker-positive cells in the dentage gyrus of control mice (white bars) and β-catenin cKO mice (black bars).

significantly reduced ($P < 0.001$) in the β-catenin cKO mice (**Supplementary Fig. 6**). In control mice, we readily observed Sox2^{CRE}GFP-positive cells that gave rise to mature neurons with extensive neurites (**Fig. 5a**). Quantification of Sox2^{CRE}GFP-positive cells in control mice revealed that ~50% of them became NeuN-positive mature granule neurons (**Fig. 5d**).

In contrast, there was a substantial decrease in Sox2^{CRE}GFP-positive cells that became mature neurons in β-catenin cKO mice (**Fig. 5a**). The percentage of NeuN and GFP double-positive cells was reduced by 85% relative to that of control mice (**Fig. 5d**). The number of Sox2^{CRE}GFP-positive cells that were also labeled by Prox-1, which labels both immature and mature neurons, was also reduced by 90% in β-catenin cKO mice compared with control mice (**Supplementary Fig. 6**).

To examine Sox2^{CRE}GFP-positive cells in the stem cell compartment, we stained the cells with GFAP, a marker of radial stem-like cells and astrocytes, and BrdU (**Fig. 6a**). The proportion of GFAP and GFP double-positive cells in β-catenin cKO mice was 4.4-fold higher than that in control mice (**Fig. 5d**). The Sox2-^{CRE}GFP-positive cells in β-catenin cKO mice were also positive for Sox2 and labeled with BrdU (**Fig. 6b**). There was no substantial change in the number of GFP and Sox2 double-positive cells (**Fig. 5c**). The proportion of GFP and Sox2 double-positive cells was 1.5-fold higher than that in control mice (**Fig. 5d**).

We observed similar results with a lentivirus approach *in vivo*. Cells that were positive for the lentivirus encoding β-catenin shRNA and GFP cells did not significantly colocalize with NeuroD1-positive cells ($P < 0.001$), whereas control lentivirus-GFP–positive cells colocalized with many NeuroD1-positive cells (**Fig. 7** and **Supplementary Fig. 7**). Cells infected with a lentivirus expressing shRNA specific to β-catenin were positive for Sox2 and BrdU, similar to cells infected with a control lentivirus expressing GFP (**Supplementary Fig. 8**). The shRNA-GFP–positive cells colocalized with GFAP-positive cells and Nestin-positive cells (Nestin is a radial glial cell marker) (**Supplementary Fig. 9**). These data suggest that the maintenance of the undifferentiated stem cell compartment and, to a large extent, astrocytic lineage cells and/or GFAP-positive radial stem-like cells remained intact with knockdown of β-catenin. Together, these data indicate that Sox2-positive cells cannot transition to immature and mature granule neurons when Wnt/β-catenin signaling is blocked, whereas the stem/progenitor cell compartment remains intact.

Wnt is important for survival of neuronal progenitor cells

The decrease of Sox2^{CRE}GFP-positive cells in β-catenin cKO mice could also be explained by a defect in the survival of neuronal progenitors. Thus, we examined the presence of dead and/or dying cells by activated caspase 3 (AC3) staining. We found more AC3-positive cells in dentate gyrus of β-catenin cKO mice than in control mice (**Fig. 6c,d**). Although we observed AC3-positive cells that colabeled

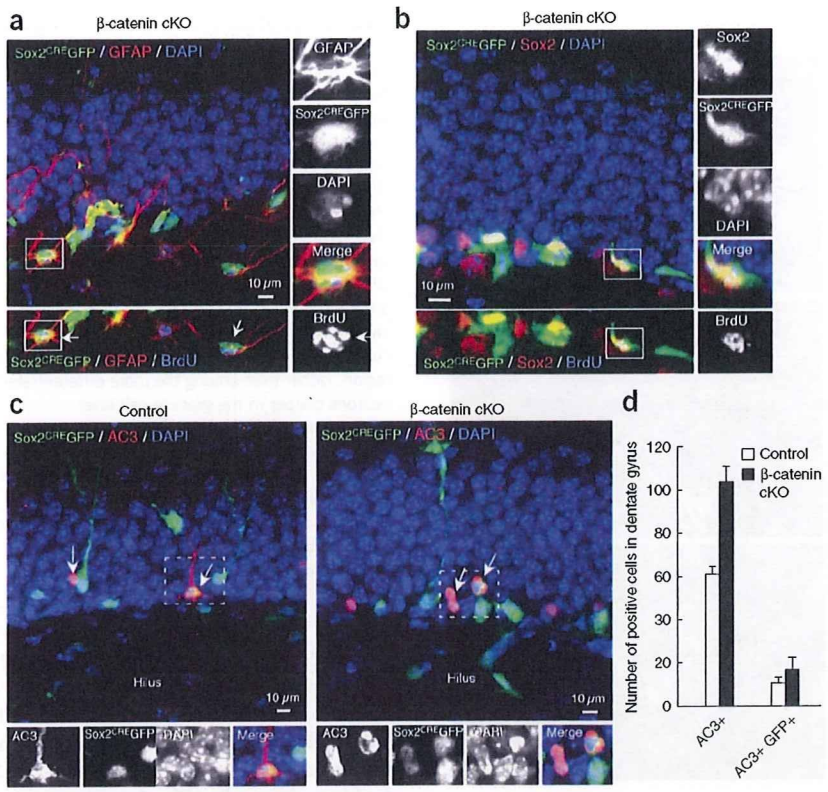

Figure 6 Lineage tracing Sox2-positive NSCs in β-catenin cKO mice. Immunohistochemical analysis of the Sox2^{CRE}GFP cells. (**a**,**b**) Sox2-positive cells were able to give rise to GFAP-positive (red, **a**) and to Sox2-positive NSCs (red, **b**). Magnified images show triple immunohistochemistry of GFAP (**a**) or Sox2 (**b**), GFP (green) and BrdU (blue, lower panels). (**c**) Immunohistochemical analysis of apoptotic cells labeled by AC3 in β-catenin cKO mice. Representative image of AC3 (red), GFP (green) and DAPI (blue) in control mice (left) and β-catenin cKO mice (right). The GFP-positive cells colocalizing with the AC3-positive cells are indicated by white arrows. The GFP and AC3 double-positive cells in the white dotted square are magnified in the bottom panels. (**d**) Quantification of GFP-positive and AC3-positive cells in dentate gyrus of control and β-catenin cKO mice. The numbers of the AC3-positive and AC3 and GFP double-positive cells in the dentate gyrus of control mice (white bars) and β-catenin cKO mice (black bars) are plotted.

with Sox2 (**Supplementary Fig. 10**), the total number of Sox2-positive cells remained unchanged in β-catenin cKO mice (**Fig. 5c**), suggesting that inhibition of Wnt/β-catenin signaling in Sox2-positive NSCs is important for the generation NeuroD1-positive cells from Sox2-positive NSCs, as well as for the survival of neuronal progenitors.

Finally, to examine whether Wnt/β-catenin–mediated neuronal differentiation is dependent on NeuroD1, we performed loss-of-function experiments in adult NSCs expressing siRNA specific to NeuroD1, as well as in subventricular zone and dentate gyrus neurospheres from 4-week-old *Neurod1*$^{loxP/loxP}$ mice (NeuroD1 cKO) mice[15]. The addition of Wnt3a ligand induced microtubule associated protein 2AB (Map2AB) expression in neurons in NSCs that were treated with of control random siRNA; Map2AB expression was completely suppressed with the introduction of NeuroD1 siRNA (**Supplementary Fig. 11**). Moreover, Wnt3a ligand treatment in NeuroD1 cKO neurospheres[15] with control GFP lentivirus resulted in TUJ1-positive neurons after 2 d (**Supplementary Fig. 12**). However, in the presence of lentivirus expressing Cre, which caused the deletion of NeuroD1, Wnt3a stimulation failed to induce substantial numbers of TUJ1-positive neurons, which is consistent with the idea that NeuroD1 is essential for Wnt3a-mediated neuronal differentiation.

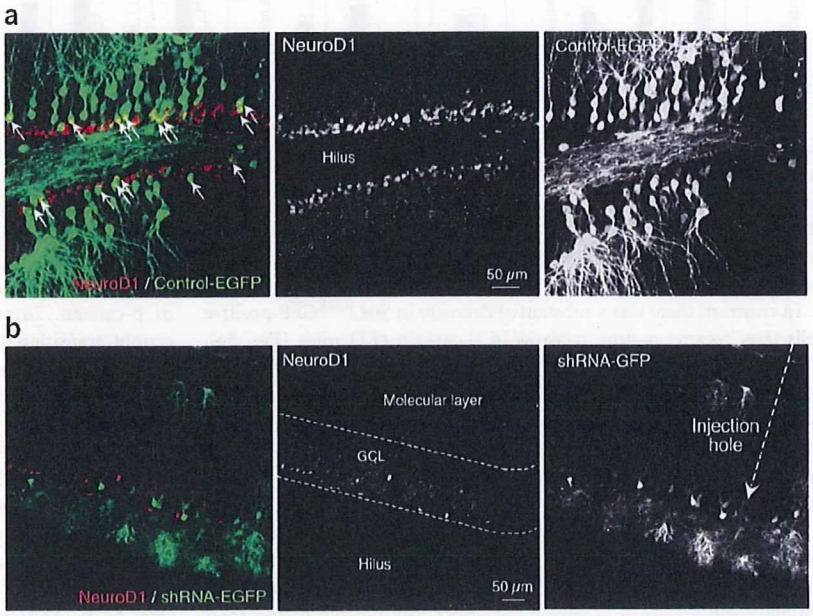

Figure 7 Infection of lentivirus expressing β-catenin shRNA *in vivo*. To evaluate the effect of Wnt signaling *in vivo*, lentivirus expressing β-catenin shRNA or control lentivirus expressing only EGFP (lentivirus-GFP) was stereotactically injected into adult rat hippocampus. (**a**) Lentivirus-GFP in dentate gyrus. White arrows indicate the population of cells that were double positive for NeuroD1 (red) and EGFP (green). (**b**) Immunohistochemical analysis of the cells infected by the lentivirus encoding β-catenin shRNA and GFP. Cells expressing β-catenin shRNA and GFP (green) and NeuroD1-positive cells (red) are shown.

LINE-1 promoter activity in newborn and mature neurons

On the basis of our results, we hypothesized that LINE-1 sequences are active during adult neurogenesis. To evaluate LINE-1–based promoter activity *in vivo*, we prepared a lentiviral vector that encodes the LINE-1

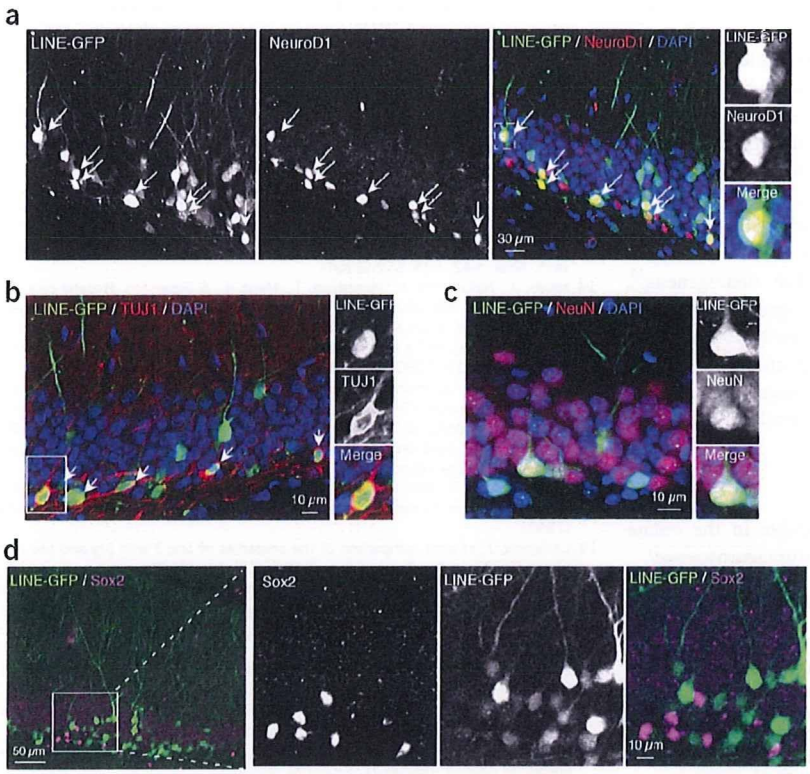

Figure 8 Activity of LINE-1 as a promoter in adult rat hippocampus. (**a**–**d**) We examined the activity and specificity of the LINE-1–based promoter in adult rat hippocampus. EGFP-expressing lentivirus, under the control of the LINE-1–based promoter, was stereotactically microinjected into the dentate gyrus of adult rats and the population of GFP-positive cells (green) was analyzed by immunohistochemistry using an antibody to NeuroD1 (red, **a**). Comparisons of the LINE-GFP population (green) to TUJ1 staining (red, **b**), NeuN staining (red, **c**) and Sox2 staining (magenta, **d**) are also shown.

ORF2 fragment fused to the *egfp* gene (LINE-GFP). LINE-GFP lentivirus was stereotactically injected into dentate gyrus of young adult rats. Notably, we observed LINE-GFP expression restricted to neurogenic areas, and GFP-positive cells colocalized with NeuroD1-positive neuronal progenitors and TUJ1-positive newborn granule neurons (**Fig. 8a,b**). Moreover, we observed a similar expression pattern of the 5′ UTR of LINE-GFP in TUJ1-positive newborn neurons in dentate gyrus (**Supplementary Fig. 13**). We also detected LINE-GFP–positive cells that migrated further into the granule cell layer, where mature neurons reside that were NeuN positive[33] (**Fig. 8c** and **Supplementary Fig. 14**). LINE-GFP–positive cells were negative for Sox2 (**Fig. 8d**). These *in vivo* data are consistent with our *in vitro* results, which indicate that NeuroD1 and LINE-1 expression are specifically induced only when Sox2-positive NSCs transition to newborn neurons on Wnt/β-catenin activation.

DISCUSSION

We found an important function for canonical Wnt/β-catenin signaling in balancing self-renewal of NSCs and neuronal differentiation in adult dentate gyrus. Our results (as summarized in **Supplementary Fig. 15**) indicate that the Sox2 and TCF/LEF regulatory element in the *Neurod1* promoter is critical for the transition from Sox2-mediated repression to Wnt/β-catenin-mediated activation, that the clear, dose-dependent activation of the *Neurod1* promoter by the Wnt3a ligand is dependent on the Sox/LEF-binding site, that deletion of β-catenin leads to substantial loss of NeuroD1-positive cells, whereas the stem cell compartment remains intact *in vivo*, and that Wnt/β-catenin–mediated neuronal differentiation is dependent on NeuroD1, at least *in vitro*. Taken together, these findings indicate that the decreased adult neurogenesis observed in the *Sox2–cre-gfp; Ctnnb1*$^{loxP/loxP}$ mice is probably a result of a failure of neuronal lineage commitment from Sox2-positive NSCs and of survival of Sox2- and NeuroD1-positive progenitor cells/neuroblasts.

During embryonic development, neurogenins function as pro-neural proteins that activate transcription of *Neurod1* through E-protein binding sites in its promoter[28–30]. However, the transcriptional/epigenetic mechanism that regulates NeuroD1 expression in the adult neurogenic niche is not clear. In the SGZ, hippocampal astrocyte–derived factors, such as Wnt proteins, signal to NSCs to promote adult neurogenesis. Among several Wnt proteins (Wnt3a, Wnt2a, Wnt5a, Wnt7a and Wnt8b)[34–36], Wnt3a has a dominant role in CNS development, as the deletion of Wnt3a (*Wnt3a*$^{-/-}$ mice) results in the absence of dentate gyrus formation[35]. Furthermore, it has been reported that β-catenin is involved in the dendritic development of newborn neurons[37]. Both canonical[4–8] and noncanonical[37] Wnt/β-catenin signaling may contribute to the step-wise progression of adult hippocampal neurogenesis by removing Sox2 repression and turning on NeuroD1. Similar to a loss of Wnt/β-catenin signaling, NeuroD1 deficiency during hippocampal development leads to a complete loss of dentate gyrus formation in mice[10,11]. In adult stages, when the hippocampal formation is fully developed, conditional deletion of β-catenin and NeuroD1 (ref. 15) lead to a similar phenotype in dentate gyrus, that is, a decreased number of neuronal progenitors/newborn neurons, suggesting that the regulation of canonical Wnt/β-catenin signaling and *Neurod1* gene expression are tightly linked and the functions of both β-catenin and NeuroD1 are indispensable for adult neurogenesis and for the survival of neuronal progenitors. Recently, it was shown that Wnt-mediated adult hippocampal neurogenesis contributed to learning and memory in rats[38]. Our data suggest that Wnt signaling activation might be a major environmental factor that is relayed to the NSC genome for neuronal lineage commitment to modulate behavior.

Our finding that the Wnt-mediated regulatory mechanism is required for the activation of NeuroD1 can be broadly extended to the regulation of LINE-1. Because retro-element sequences are scattered throughout the genome and contain Sox/LEF DNA regulatory elements, one possibility is that Sox/LEF-binding sites act as bi-directional promoters and cause nearby neuronal gene loci to become de-silenced and activated during adult neurogenesis. Thus, to explore the possibility that LINE-1 sequences containing Sox2 and TCF/LEF sites might confer cell type–specific regulation as described for NeuroD1, we searched for LINE-1 sequences proximal to the transcriptional start sites of known protein-coding genes in human, mouse and

rat genomes. We were able to identify 79, 84 and 25 such LINE-1 elements within –6,000 and +1,000 base pairs of the target human, mouse and rat genes, respectively (**Supplementary Tables 1–3**). These bioinformatics analyses suggest that there is a global regulatory mechanism for controlling the activation/repression of neuronal gene expression that uses embedded retrotransposition sequences in the genome as a putative master regulatory pathway during adult neurogenesis. However, the causal relationship between LINE-1 sequences and transcriptional activation of nearby Sox/LEF-driven neuronal genes awaits future validation. Recently, it has been shown that environment is a robust stimulator of adult neurogenesis[39], possibly through the activation of the Sox/LEF regulatory elements described here. Consistent with these data, we recently observed that voluntary exercise increased LINE-1 retrotransposition in dentate gyrus[40]. Our data provides a window into the molecular mechanism behind experience-dependent LINE-1 retrotransposition that may affect neuronal plasticity.

METHODS

Methods and any associated references are available in the online version of the paper at http://www.nature.com/natureneuroscience/.

Note: Supplementary information is available on the Nature Neuroscience website.

ACKNOWLEDGMENTS

We thank T. Ohtake for assistance with animal care and supporting our *in vivo* experiments. We thank M. Namihira and J. Kohyama for assistance in obtaining immunostaining data, E. Mosser for the constitutively active β-catenin construct, and G. Canettieri and M. Montminy for HDAC1. We thank A. Huynh for help with immunohistochemical analysis. We are grateful for the technical assistance of B. Miller and to M.L. Gage for editorial comments. T.K., M.W. and M.A. were supported by various grants from National Institute of Advanced Industrial Science and Technology. T.K. was partly supported by the Grant-in-Aid for Exploratory Research. F.H.G. was supported by grants from the US National Institutes of Health (MH082070) and the G. Harold and Leila Y. Mathers Charitable Foundation.

AUTHOR CONTRIBUTIONS

T.K., J.H., A.M., K.N. and F.H.G. conceptualized and designed the study. T.K., J.H., A.M. and F.H.G. analyzed the data. T.K. conducted the experiments with assistance from M.W., J.H. and L.M. G.Y. and A.M. conducted the bioinformatics analysis. A.M. helped design the LINE-1 plasmid constructs, D.C.L. helped with the Wnt plasmid design and constructs, and M.W. designed the shRNA construct. M.A. contributed reagents and analytical tools. T.K. wrote the paper with comments from all of the authors.

Published online at http://www.nature.com/natureneuroscience/.
Reprints and permissions information is available online at http://www.nature.com/reprintsandpermissions/.

1. Suh, H. *et al. In vivo* fate analysis reveals the multipotent and self-renewal capacities of Sox2$^+$ neural stem cells in the adult hippocampus. *Cell Stem Cell* **1**, 515–528 (2007).
2. Song, H., Stevens, C.F. & Gage, F.H. Astroglia induce neurogenesis from adult neural stem cells. *Nature* **417**, 39–44 (2002).
3. Barkho, B.Z. *et al.* Identification of astrocyte-expressed factors that modulate neural stem/progenitor cell differentiation. *Stem Cells Dev.* **15**, 407–421 (2006).
4. Lie, D.C. *et al.* Wnt signaling regulates adult hippocampal neurogenesis. *Nature* **437**, 1370–1375 (2005).
5. Galceran, J., Miyashita-Lin, E.M., Devaney, E., Rubenstein, J.L. & Grosschedl, R. Hippocampus development and generation of dentate gyrus granule cells is regulated by LEF1. *Development* **127**, 469–482 (2000).
6. Machon, O., van den Bout, C.J., Backman, M., Kemler, R. & Krauss, S. Role of beta-catenin in the developing cortical and hippocampal neuroepithelium. *Neuroscience* **122**, 129–143 (2003).
7. Solberg, N., Machon, O. & Krauss, S. Effect of canonical Wnt inhibition in the neurogenic cortex, hippocampus and premigratory dentate gyrus progenitor pool. *Dev. Dyn.* **237**, 1799–1811 (2008).
8. Wexler, E.M., Geschwind, D.H. & Palmer, T.D. Lithium regulates adult hippocampal progenitor development through canonical Wnt pathway activation. *Mol. Psychiatry* **13**, 285–292 (2008).
9. Clevers, H. Wnt/β-catenin signaling in development and disease. *Cell* **127**, 469–480 (2006).
10. Miyata, T., Maeda, T. & Lee, J.E. NeuroD is required for differentiation of the granule cells in the cerebellum and hippocampus. *Genes Dev.* **13**, 1647–1652 (1999).
11. Liu, M. *et al.* Loss of BETA2/NeuroD leads to malformation of the dentate gyrus and epilepsy. *Proc. Natl. Acad. Sci. USA* **97**, 865–870 (2000).
12. Tozuka, Y., Fukuda, S., Namba, T., Seki, T. & Hisatsune, T. GABAergic excitation promotes neuronal differentiation in adult hippocampal progenitor cells. *Neuron* **47**, 803–815 (2005).
13. Deisseroth, K. *et al.* Excitation-neurogenesis coupling in adult neural stem/progenitor cells. *Neuron* **42**, 535–552 (2004).
14. Hsieh, J., Nakashima, K., Kuwabara, T., Mejia, E. & Gage, F.H. Histone deacetylase inhibition–mediated neuronal differentiation of multipotent adult neural progenitor cells. *Proc. Natl. Acad. Sci. USA* **101**, 16659–16664 (2004).
15. Gao, Z. *et al. Neurod1* is essential for the survival and maturation of adult-born neurons. *Nat. Neurosci.* **12**, 1090–1092 (2009).
16. Nishimoto, M., Fukushima, A., Okuda, A. & Muramatsu, M. The gene for the embryonic stem cell coactivator UTF1 carries a regulatory element which selectively interacts with a complex composed of Oct-3/4 and Sox-2. *Mol. Cell. Biol.* **19**, 5453–5465 (1999).
17. Ferri, A.L. *et al.* Sox2 deficiency causes neurodegeneration and impaired neurogenesis in the adult mouse brain. *Development* **131**, 3805–3819 (2004).
18. Yuan, H., Corbi, N., Basilico, C. & Dailey, L. Developmental-specific activity of the FGF-4 enhancer requires the synergistic action of Sox2 and Oct-3. *Genes Dev.* **9**, 2635–2645 (1995).
19. Collignon, J. *et al.* A comparison of the properties of Sox-3 with Sry and two related genes, Sox-1 and Sox-2. *Development* **122**, 509–520 (1996).
20. Ambrosetti, D.C., Basilico, C. & Dailey, L. Synergistic activation of the fibroblast growth factor 4 enhancer by Sox2 and Oct-3 depends on protein-protein interactions facilitated by a specific spatial arrangement of factor binding sites. *Mol. Cell. Biol.* **17**, 6321–6329 (1997).
21. Avilion, A.A. *et al.* Multipotent cell lineages in early mouse development depend on SOX2 function. *Genes Dev.* **17**, 126–140 (2003).
22. Bylund, M., Andersson, E., Novitch, B.G. & Muhr, J. Vertebrate neurogenesis is counteracted by Sox1–3 activity. *Nat. Neurosci.* **6**, 1162–1168 (2003).
23. Graham, V., Khudyakov, J., Ellis, P. & Pevny, L. SOX2 functions to maintain neural progenitor identity. *Neuron* **39**, 749–765 (2003).
24. Bani-Yaghoub, M. *et al.* Role of Sox2 in the development of the mouse neocortex. *Dev. Biol.* **295**, 52–66 (2006).
25. Muotri, A.R. *et al.* Somatic mosaicism in neuronal precursor cells mediated by L1 retrotransposition. *Nature* **435**, 903–910 (2005).
26. D'Amour, K.A. & Gage, F.H. Genetic and functional differences between multipotent neural and pluripotent embryonic stem cells. *Proc. Natl. Acad. Sci. USA* **100**, 11866–11872 (2003).
27. Gage, F.H. *et al.* Survival and differentiation of adult neuronal progenitor cells transplanted to the adult brain. *Proc. Natl. Acad. Sci. USA* **92**, 11879–11883 (1995).
28. Ma, Q., Kintner, C. & Anderson, D.J. Identification of *neurogenin*, a vertebrate neuronal determination gene. *Cell* **87**, 43–52 (1996).
29. Farah, M.H. *et al.* Generation of neurons by transient expression of neural bHLH proteins in mammalian cells. *Development* **127**, 693–702 (2000).
30. Guillemot, F. Vertebrate bHLH genes and the determination of neuronal fates. *Exp. Cell Res.* **253**, 357–364 (1999).
31. Hsieh, J. & Gage, F.H. Chromatin remodeling in neural development and plasticity. *Curr. Opin. Cell Biol.* **17**, 664–671 (2005).
32. Brault, V. *et al.* Inactivation of the β-catenin gene by Wnt1-Cre–mediated deletion results in dramatic brain malformation and failure of craniofacial development. *Development* **128**, 1253–1264 (2001).
33. Yang, N., Zhang, L., Zhang, Y. & Kazazian, H.H., Jr. An important role for RUNX3 in human LINE-1 transcription and retrotransposition. *Nucleic Acids Res.* **31**, 4929–4940 (2003).
34. Grove, E.A., Tole, S., Limon, J., Yip, L. & Ragsdale, C.W. The hem of the embryonic cerebral cortex is defined by the expression of multiple Wnt genes and is compromised in Gli3-deficient mice. *Development* **125**, 2315–2325 (1998).
35. Lee, S.M., Tole, S., Grove, E. & McMahon, A.P. A local Wnt-3a signal is required for development of the mammalian hippocampus. *Development* **127**, 457–467 (2000).
36. Shimogori, T., VanSant, J., Paik, E. & Grove, E.A. Members of the Wnt, Fz and Frp gene families expressed in postnatal mouse cerebral cortex. *J. Comp. Neurol.* **473**, 496–510 (2004).
37. Gao, X., Arlotta, P., Macklis, J.D. & Chen, J. Conditional knock-out of beta-catenin in postnatal-born dentate gyrus granule neurons results in dendritic malformation. *J. Neurosci.* **27**, 14317–14325 (2007).
38. Jessberger, S. *et al.* Dentate gyrus–specific knockdown of adult neurogenesis impairs spatial and object recognition memory in adult rats. *Learn. Mem.* **16**, 147–154 (2009).
39. van Praag, H., Shubert, T., Zhao, C. & Gage, F.H. Exercise enhances learning and hippocampal neurogenesis in aged mice. *J. Neurosci.* **25**, 8680–8685 (2005).
40. Muotri, A.R., Zhao, C., Marchetto, M.C.N. & Gage, F.H. Environmental influence on L1 retrotransposons in the adult hippocampus. *Hippocampus* (in press).

ONLINE METHODS

Cell culture. Adult hippocampal NSCs were cultured as described[27]. Adult NSCs were cultured with Dulbecco's modified Eagle's medium/F-12 medium (Invitrogen) containing 20 ng mL^{-1} FGF-2 (Wako), 1% N_2 supplement (Invitrogen), 1% antibiotic-antimycotic (Invitrogen), and 2 mM L-glutamine (Wako) in a 5% CO_2 incubator at 37 °C. For neuronal differentiation, cells were cultured in N2 medium (Invitrogen) containing retinoic acid (1 μM, Sigma), forskolin (5 μM, Sigma) and KCl (40 mM, Wako). Dkk1 (500 ng mL^{-1}, R&D Systems), Wnt3a (50 ng mL^{-1}, R&D Systems) and 5 μM TDZD8 (4-benzyl-2-methyl-1,2,4-thiadiazolidine-3,5-dione, Calbiochem) were added to the medium to determine the effects of Wnt signaling. For the adult neurosphere culture from ND1 cKO mice (**Supplementary Fig. 12**), spheres were cultured on uncoated dishes. Lentivirus expressing GFP or Cre-GFP was introduced to the neurospheres. To examine the effect of Wnt signaling on *Neurod1*$^{-/-}$cells (neurospheres), we added Wnt3a ligand (50 ng mL^{-1}) for 2 d after the removal of FGF2 and epidermal growth factor 2.

Construction of plasmids, shRNA and siRNA. Five copies of the Sox/LEF-binding sites were fused upstream to the 200-bp cytomegalovirus (CMV) minimal promoter carrying a TATA box and linked to the *luciferase* gene (Sox/LEF-TATA). Five copies of the DNA binding sequence for Sox2 (Sox-TATA) and five copies of the DNA binding sequence for TCF/LEF (LEF-TATA) were also fused to the minimal promoter-driven luciferase. The mutant construct containing *Neurod1* promoter–driven *luciferase* (NeuroD1 mutant luciferase in **Fig. 2e**) was designed to contain a mutation in the Sox/LEF site to abolish Sox2 and TCF/LEF binding (AAC AAA G sequence was exchanged to GCT AGC G). The Wnt3, DnWnt, Sox2, HDAC1 and β-catenin–expressing lentiviral vectors were constructed using CSC PW, a third-generation, self-inactivating lentiviral vector[41]. Each expression cassette was subcloned at the 3′ end of the CMV promoter on CSC SP PW. The shRNA for the *Ctnnb1* gene was designed to target the sequence GCA ATC AGC TGG CCT GGT TTG, located in the last exon of the rat β-catenin transcript. It was constructed by connecting a shRNA sequence with a terminator under the murine *U6* promoter. This shRNA cassette was subcloned into the TUHSA CS PW lentiviral vector, which contains cassettes of CMV-EGFP, with the ClaI and PmeI restriction sites, and the U6 promoter with the ClaI and HpaI sites. TUHSA CS PW lentiviral vector was derived from the original CSC SP PW plasmid. The knockdown effect of the *Ctnnb1* shRNA was confirmed by western blot analysis using cell lysate from lentivirus-infected, GFP-positive adult hippocampal NSCs (**Supplementary Fig. 2**). The production of lentivirus has been described elsewhere[42]; the viral titers were greater than 1.5×10^4 transducing units ng^{-1}, as determined by the p24 ELISA assay. The murine *Neurod1* promoter was cloned by PCR from genomic DNA and inserted into CSC PW-Luci at the site of the CMV promoter using the restriction enzyme sites for ClaI and BamHI. Sox-TATA, Sox/LEF-TATA and LEF-TATA luciferase reporter plasmids included the binding sequences of the Sox transcription factor (AAC AAT Gtt tAA CAA TGa aaA ACA ATG ttt TAC AAT Gaa aAT ATC AAT G, where capital letters indicate binding sequences and lowercase letters indicate linker sequences), the Sox and LEF transcription factor (AAC AAA Gtt aAA CAA AGt ttA ACA AAG aaa AAC AAA Gta tAA CAA AG), and the LEF transcription factor (AAC AAA aaa AAC AAA ttt AAC AAA aaa AAC AAA ttt AAC AAA). Synthetic siRNAs targeting *Neurog1*, *Neurog2*, *Ctnnb1* and *Neurod1* rat mRNA were purchased from Ambion (Silencer Select siRNA). The siRNA-targeting Sox2 was custom-synthesized by Ambion (custom Select siRNA).

Immunofluorescence studies. Immunofluorescence studies were performed as described[27]. We used mouse monoclonal antibody to beta-tubulin III (TUJ1, 1:500, Promega), antibody to Sox2 (1:300, Chemicon), goat antibody to NeuroD (1:100, Santa Cruz Biotechnology), mouse antibody to nestin (BD Biosciences), guinea pig antibody to GFAP (1:500, Advanced Immunochemical), mouse antibody to NeuN (1:60, clone A10), mouse monoclonal antibody to Wnt3a (1:100, Abcam), goat antibody to Wnt3 (1:100, Everest), mouse monoclonal antibody to S100β (1:200, Abcam), rabbit monoclonal antibody to calretinin (1:100, Abcam), rabbit antibody to Ki67 (1:150, Abcam), rabbit antibody to doublecortin (1:100, Santa Cruz Biotechnology), rabbit antibody to RUNX3 (1:250, Abcam), rat antibody to BrdU (1:250, Abcam) and DAPI (Wako). To examine the proliferative status of NeuroD1-expressing cells (**Fig. 1**), we injected Fisher 344 rats (7–8-week-old rats) with BrdU (100 mg per kg) once a day for 1 week and used the brain sections for BrdU staining analysis. For the immunostaining analysis of AC3 (**Fig. 6**), additional pretreatment of brain sections was conducted[15]. All secondary antibodies were from Jackson ImmunoResearch. Images were analyzed using a Bio-Rad Radiance confocal imaging system or Carl Zeiss LSM confocal imaging system.

qRT-PCR assays. For qRT-PCR assays, total RNA was extracted from cells by Isogen (Nippon Gene). After DNase I treatment (TURBO DNA-free, Ambion), cDNA was synthesized from 1 μg of purified RNA by the SuperScript II First-Strand cDNA synthesis system (Invitrogen), according to the manufacturer's instructions. qRT-PCR was performed with a real-time PCR machine (Bio-Rad). The reported results of the qRT-PCR assays are the averages of two independent RNA preparations. The PCR cycling parameters were 94 °C for 2 min, 40 cycles at 94 °C for 15 s, 60 °C for 20 s and 72 °C for 40 s. Data analysis was performed using the comparative threshold cycle value (C_t) method.

Luciferase assay. Adult NSCs were electroporated with reporter plasmids by a nucleofector device (Amaxa). *Neurod1-luciferase* in a pGL2-luci plasmid (or mutant *Neurod1-luciferase*) and renilla luciferase (R-luc) as an internal control were co-electroporated into adult NSCs. We measured luciferase activity 48 h after electroporation in 50 μL of lysis supernatant with the Dual-Luciferase Reporter Assay System (Promega) according to the manufacturer's protocol. The luminescence signal was quantified with a luminometer (Lumant LB 9501). The ORF2 region and 5′ UTR of human LINE-1.3 were cloned and inserted into CSC PW (the same constructs were used for the EGFP reporter in **Fig. 8**) at the site of the CMV promoter and into the pGL2-luci plasmid.

ChIP and RT-PCR. ChIP was performed using a kit following the manufacturer's protocol (Upstate). Chromatin from cell extracts (input) or immunoprecipitated with specific antibodies was amplified by PCR using primers designed to flank the Sox/LEF-binding site in the rat *Neurod1* promoter and LINE-1. For primary antibodies, we used antibody to HDAC1 (rabbit, Upstate), antibody to acetyl-histone H4 (rabbit, Upstate), antibody to acetyl-histone H3 (rabbit, Upstate), antibody to dimethyl-histone H3 (Lys4, mouse, Upstate), antibody to dimethyl-histone H3 (Lys9, mouse, Upstate), antibody to Sox2 (rabbit, Chemicon) and antibody to β-catenin (rabbit, Cell Signaling). RT-PCR was performed using total RNA extracted from adult hippocampus NSCs. A total of 1 μg RNA was used for first-strand cDNA synthesis with SuperScript II (GibcoBRL). PCR primer sequences are available on request.

Bioinformatics analysis. The genomic sequences for rat (rn3), human (hg17) and mouse (mm5) and the species-specific annotation for known protein coding genes and LINEs (annotated with RepeatMasker) were obtained from the University of California Santa Cruz public genome database (http://genome.ucsc.edu). Candidate binding sites for Sox2 (WWC AAW G) and TCF/LEF (WWC AAA) were identified on either strand of genomic sequence (W for either A or T and N for either A, C, G or T). Promoters were defined as the regions 6,000 bases upstream and 1,000 bases downstream of the annotated transcriptional start sites of protein coding genes. Full-length (at least 6 kb) LINE elements containing TCF/LEF or Sox2 candidate sites located in promoters were retained. We identified 79, 84 and 25 such LINE elements in the human, mouse and rat genomes, respectively (**Supplementary Tables 1–3**).

Retrovirus injection into adult hippocampus. All animal procedures were performed in accordance with protocols approved by the Institutional Animal Care and Use Committee of the National Institute of Advanced Industrial Science and Technology. We used retrovirus expressing a Cre-GFP fusion protein under the control of the *Sox2* promoter[1,26] ($Sox2^{CRE}GFP$). It has been determined that *Sox2* promoter (3.1 kb) on the retrovirus recapitulates endogenous Sox2 expression similarly in CNS[1]. *Rosa26-egfp* mice (Jackson Laboratory), harboring *egfp* and a *loxP*-flanked stop codon, were crossed with $Ctnnb1^{loxP/loxP}$ mice (Jackson Laboratory). The $Ctnnb1^{loxP/loxP}$ allele contains *loxP* sites flanking exons 2–6 and has been shown to be a conditional null allele[32]. Transduction of Cre recombinase under the *Sox2* promoter deleted the

doi:10.1038/nn.2360

stop codon to activate GFP expression in Sox2-positive cells (control mice). We injected Sox2^{CRE}GFP retrovirus into *Ctnnb1*$^{loxP/loxP}$ mice that were crossed with a *Rosa26-egfp* reporter line and traced GFP-positive cells that had stem cell–specific deletion of *Ctnnb1*$^{loxP/loxP}$ (β-catenin cKO mice). The retrovirus (1.0–1.5 μL) was injected into either control (*Rosa26-egfp*) or *Ctnnb1*$^{loxP/loxP}$; *Rosa26-egfp* mice ($n = 6$ per group). The retrovirus was stereotactically injected into the dentate gyrus of the hippocampus (anterioposterior −2.5 mm, lateral ±2.0 mm and dorsoventral −2.0 to 2.5 mm from Bregma) with a 26-gauge stainless microinjection needle at a rate of 0.5 μl min^{-1}. The needle remained in place for an additional 2 min to facilitate delivery of the virus. Starting 2 weeks after the retrovirus injection, we injected BrdU (100 mg per kg) once a day for 2 weeks. We killed the mice 3 weeks post-surgery and perfused them with 4% paraformaldehyde solution. Brain sections were cut at a thickness of 30 μm with a microtome (ROM-380, Yamato). An immunohistochemical analysis was performed using a confocal microscope.

Lentivirus injection into adult rat hippocampus. Concentrated lentivirus (1.5 μl) was injected stereotactically into the dentate gyrus of the hippocampus (anterioposterior −3.5 mm, lateral ±2.5 mm and dorsoventral −3.5 mm from Bregma) of adult female CD (Sprague-Dawley [SD]) rats (6–8 weeks old, $n = 6$ per group; **Fig. 5**) with a 26-gauge stainless microinjection needle at a rate of 0.5 μl min^{-1}. To assess LINE-1 promoter activity with lentivirus encoding the LINE-1 ORF2 fragment fused to *gfp* (LINE-GFP; **Fig. 8**), we stereotactically injected lentivirus aliquots injected into the dentate gyrus of young adult rats (7–8 weeks old, $n = 6$). The needle remained in place for an additional 2 min to facilitate delivery of the virus. We injected BrdU (100 mg per kg) once a day for 1 week starting 2 weeks after the initial injection of the virus. The rats were killed 3 weeks post-infection and perfused with 4% paraformaldehyde. Brain sections were cut at a thickness of 30 μm with a microtome (ROM-380, Yamato). An immunohistochemical analysis was performed using a confocal microscope.

41. Miyoshi, H., Takahashi, M., Gage, F.H. & Verma, I.M. Stable and efficient gene transfer into the retina using an HIV-based lentiviral vector. *Proc. Natl. Acad. Sci. USA* **94**, 10319–10323 (1997).
42. Pfeifer, A., Brandon, E.P., Kootstra, N., Gage, F.H. & Verma, I.M. Delivery of the Cre recombinase by a self-deleting lentiviral vector: efficient gene targeting *in vivo*. *Proc. Natl. Acad. Sci. USA* **98**, 11450–11455 (2001).

Experimental Neurology 219 (2009) 104–111

Contents lists available at ScienceDirect

Experimental Neurology

journal homepage: www.elsevier.com/locate/yexnr

Neuronal differentiation of neural precursor cells is promoted by the methyl-CpG-binding protein MeCP2

Keita Tsujimura, Masahiko Abematsu, Jun Kohyama, Masakazu Namihira, Kinichi Nakashima *

Laboratory of Molecular Neuroscience, Graduate School of Biological Sciences, Nara Institute of Science and Technology, 8916-5, Takayama, Ikoma, Nara 630-0101, Japan

ARTICLE INFO

Article history:
Received 27 December 2008
Revised 2 April 2009
Accepted 2 May 2009
Available online 8 May 2009

Keywords:
MeCP2
Rett syndrome
Epigenetics
Differentiation
Neural stem cells
Cytokine
Transplantation

ABSTRACT

Methyl-CpG-binding protein 2 (MeCP2), a methyl-CpG-binding domain protein family member which is expressed predominantly in neurons in the nervous system, acts as a transcriptional repressor by binding to methylated genes, and mutations in *mecp2* cause the neurological disorder known as Rett syndrome (RTT). Although MeCP2 has been reported to regulate neuronal maturation rather than fate specification of neural precursor cells (NPCs), we have previously shown that it inhibits astrocyte differentiation of NPCs when ectopically expressed. Here, we show that expression of MeCP2 in NPCs not only suppresses astrocytic differentiation but actually promotes neuronal differentiation, even in the presence of well-known astrocyte-inducing cytokines. This dual function of MeCP2 was abolished by the MEK inhibitor U0126. Moreover, we observed that a truncated form of MeCP2 found in RTT patients fails to promote neuronal differentiation. We further demonstrate that transplanted MeCP2-expressing NPCs differentiate *in vivo* into neurons in two non-neurogenic regions, striatum and spinal cord. These results suggest a possible therapeutic application for MeCP2 in neurodegenerative diseases and injuries to the central nervous system.

Introduction

Neural stem and precursor cells (NSCs/NPCs) are defined as cells that can self-renew and can give rise to the three major cell types in the nervous system: neurons, astrocytes, and oligodendrocytes (Gage, 2000). Specification of NSC/NPC lineages is regulated by cell-external cues and cell-intrinsic programs (Edlund and Jessell, 1999; Hsieh and Gage, 2004).

Cell-external cues include various types of cytokines whose signals are transduced into the nucleus with the mediation of transcription factors. Leukemia inhibitory factor (LIF), a member of the interleukin-6 (IL-6) family of cytokines that share gp130 as a signal-transducing receptor component, can effectively induce astrocyte differentiation via the Janus kinase (JAK)-signal transducer and activator of transcription (STAT) signaling pathway (Bonni et al., 1997; Nakashima et al., 1999a,b; Rajan and McKay, 1998). Bone morphogenetic proteins (BMPs), which belong to the transforming growth factor β superfamily, also induce astrocytic differentiation of NPCs (Gomes et al., 2003; Gross et al., 1996; Nakashima et al., 2001).

Cell-intrinsic programs involve epigenetic changes such as DNA methylation and histone modifications. DNA methylation at the dinucleotide CpG is one of the best-studied epigenetic modifications in multicellular genomes (Bird, 2002). NPCs at midgestation differentiate only into neurons and not into astrocytes (Qian et al., 2000), even when stimulated by LIF, due to DNA hyper-methylation in the promoter regions of astrocyte-specific genes such as glial fibrillary acidic protein (*gfap*) (Fan et al., 2005; Namihira et al., 2004; Takizawa et al., 2001). As gestation proceeds, these promoters become demethylated, enabling NPCs to differentiate into astrocytes at a later stage of development. Although late-gestational NPCs, whose astrocytic gene promoters have already become demethylated, can still give rise to neurons, these neurons do not respond to astrocyte-inducing cytokines to express *gfap* (Kohyama et al., 2008; Setoguchi et al., 2006).

Methyl-CpG-binding protein 2 (MeCP2) belongs to the methyl-CpG-binding domain (MBD) protein family, whose members function as transcriptional repressors by binding to methylated DNA (Klose and Bird, 2006; Meehan et al., 1992). MeCP2 binds to a single symmetrically methylated CpG dinucleotide via its MBD, and silences genes via its transcriptional repression domain (TRD) (Jones et al., 1998; Nan et al., 1998). MBD proteins including MeCP2 are expressed predominantly in neurons in the mammalian central nervous system (CNS) (Jung et al., 2002; Shahbazian et al., 2002). Mutations in *mecp2* cause Rett syndrome (RTT), a neurodevelopmental disorder characterized by mental retardation, motor dysfunction and autistic behavior. Recently, it was reported that MeCP2 is involved in neuronal maturation rather than cell fate decisions (Kishi and Macklis, 2004), although another study suggested that MeCP2 also plays a role in cell fate decisions during primary neurogenesis in *Xenopus* embryos by recruiting the transcription repressor complex (Stancheva et al., 2003).

* Corresponding author. Fax: +81 743 72 5479.
E-mail address: kin@bs.naist.jp (K. Nakashima).

0014-4886/$ – see front matter © 2009 Elsevier Inc. All rights reserved.
doi:10.1016/j.expneurol.2009.05.001

We have previously shown that MeCP2 prevents the conversion of neurons to astrocytes by binding to highly methylated regions encompassing the transcription initiation sites of astrocytic genes (Kohyama et al., 2008; Setoguchi et al., 2006). Here, we show that ectopic MeCP2 expression in late-gestational NPCs inhibits astrocytic differentiation and promotes neuronal differentiation, even in the presence of astrocyte-inducing cytokines. Inhibition of the Ras-extracellular signal-regulated kinase (ERK) pathway with a MEK inhibitor abolished these MeCP2 effects. A mutant form of MeCP2, R168X, which occurs with high incidence in RTT patients, could not promote neuronal differentiation of NPCs. We further demonstrate that MeCP2 can enhance neuronal differentiation of NPCs transplanted into non-neurogenic CNS tissue *in vivo*.

Experimental procedures

NPC culture

Time-pregnant ICR mice were used to prepare NPCs. The experimental protocols described below were performed according to the animal experimentation guidelines of Nara Institute of Science and Technology. NPCs were prepared from telencephalons of E14.5 mice and cultured as described previously (Nakashima et al., 1999a,b). Briefly, the telencephalons were triturated in Hank's balanced salt solution (HBSS) by mild pipetting with a 1-ml pipet tip (Gilson, Middleton, WI, USA). Dissociated cells were cultured for 4 days prior to each experiment in N2-supplemented Dulbecco's modified Eagle's medium with F12 (Gibco, Grand Island, NY, USA) containing 10 ng/ml basic fibroblast growth factor (bFGF; R and D Systems, Minneapolis, MN, USA; N2/DMEM/F12/bFGF) on culture dishes (Nunc, Naperville, IL, USA) or chamber slides (Nunc) that had been precoated with poly-L-ornithine (Sigma, St. Louis, MO, USA) and fibronectin (Sigma).

Inhibitor experiment

U0126 (Calbiochem, Darmstadt, Germany) was dissolved in dimethyl sulfoxide (DMSO) at 10 mM, and stored at −20 °C. At the time of treatment, stocks of the inhibitor were thawed, prediluted in medium, and then added to the well up to 8 μM.

Immunocytochemistry

Cells cultured on coated chamber slides were washed with phosphate-buffered saline (PBS), fixed in 4% paraformaldehyde in PBS, and stained with combinations of the following primary antibodies: chick anti-green fluorescent protein (GFP) (1:1000; Aves Labs, Tigard, OR, USA), rabbit anti-GFP (1:1000; MBL, Nagoya, Japan), rabbit anti-βIII-tubulin (Tuj1; 1:1000; Covance, Berkeley, CA, USA), mouse anti-microtubule-associated proteins 2a and 2b (MAP2ab; 1:250; Sigma), guinea pig anti-GFAP (1:2500; Advanced Immunochemical, Long Beach, CA, USA), goat anti-doublecortin (DCX) (1:1000; Santa Cruz Biotechnology, Santa Cruz, CA, USA), mouse anti-S100β (1:1000; Sigma), rabbit anti-aquaporin 4 (AQP4) (1:500; Santa Cruz), chick anti-myelin basic protein (MBP) (1:200; Aves Labs), mouse anti-Nestin (1:1000; Chemicon, Temecula, CA, USA), rabbit anti-cleaved-caspase3 (1:1000; Cell Signaling, Danvers, MA, USA), and mouse anti-Ki67 (1:1000; BD, Franklin Lakes, NJ, USA). The following secondary antibodies were used: FITC-conjugated donkey anti-chick IgY (1:500; Jackson ImmunoResearch, West Grove, PA, USA), Cy3-conjugated donkey anti-mouse IgG (1:500; Chemicon), Cy3-conjugated donkey anti-rabbit IgG (1:500; Jackson ImmunoResearch), Alexa488-conjugated donkey anti-rabbit (1:500; Molecular Probes, Eugene, OR, USA), and Cy5-conjugated donkey anti-guinea pig (1:500; Jackson ImmunoResearch). Nuclei were stained using bisbenzimide H33258 fluorochrome trihydrochloride (Nacalai Tesque, Kyoto, Japan).

Immunohistochemistry

Brains and spinal cords from mice transcardially perfused with PBS followed by 4% paraformaldehyde were dissected, post-fixed overnight at 4 °C, and then transferred to 20% sucrose in PBS for 24 h at 4 °C. Brains and spinal cords were sectioned at 40 μm with a cryostat (Leica, Tokyo, Japan). Sections were stained with combinations of the following primary antibodies: rabbit anti-GFP (1:1000; MBL, Nagoya, Japan), goat anti-DCX (1:1000; Santa Cruz), and guinea pig anti-GFAP (1:2500; Advanced Immunochemical). The following secondary antibodies were used: Cy3-conjugated donkey anti-goat IgG (1:500; Jackson ImmunoResearch), Alexa488-conjugated donkey anti-rabbit (1:500; Molecular Probes), and Cy5-conjugated donkey anti-guinea pig (1:500; Chemicon). Nuclei were stained using bisbenzimide H33258 fluorochrome trihydrochloride (Nacalai Tesque).

Recombinant retrovirus construction and infection

Rat *mecp2* and *mecp2* (R168X) cDNAs were cloned into the expression vector pMY containing an internal ribosome entry site upstream of the GFP gene (Morita et al., 2000). The Plat-E packaging cell line was transiently transfected with these constructs using Trans-IT 293 (Mirus, Madison, WI, USA) (Morita et al., 2000). On the following day, the medium was replaced with N2/DMEM/F12/bFGF, and the cells were cultured in this medium for 1 day before virus was collected.

Transplantation into striatum

Adult ICR mice were anesthetized by intraperitoneal injection of ketamine (100 mg/kg) and xylazine (10 mg/kg). Mice were stereotaxically injected, with 2 μl of N2-supplemented DMEM/F12 medium containing 10^6 NPCs infected with retroviruses expressing GFP or GFP together with MeCP2, into the striatum (coordinates from bregma were 0 mm posterior, 2 mm lateral and 2.9 mm deep from the brain surface) using a stereotaxic apparatus (Narishige, Tokyo, Japan).

Transplantation into spinal cord

Adult ICR mice were anesthetized as above. After laminectomy at the ninth and tenth thoracic spinal vertebrae, we exposed the dorsal surface of the dura mater. Two μl of N2-supplemented DMEM/F12 medium containing 10^6 NPCs was transplanted into the spinal cord using a microinjector (Narishige).

Results

MeCP2 promotes neuronal differentiation even in the presence of astrocyte-inducing cytokines

We have previously shown that ectopic expression of MeCP2 in NPCs suppresses astrocytic differentiation induced by LIF (Kohyama et al., 2008; Setoguchi et al., 2006). In light of this finding, we anticipated that MeCP2 would also be able to influence neuronal differentiation of NPCs. To test this, we expressed GFP alone (control) and GFP together with MeCP2 by retroviral infection in E14.5 NPCs (Fig. 1A). We first examined the effect of MeCP2 in the absence of astrocyte-inducing cytokine. Ectopically expressed MeCP2 was able to enhance neuronal differentiation compared to the control during a 4-day culture after virus infection (Figs. 1B and C). The percentages of cells positive for markers of astrocytes (GFAP), oligodendrocytes (MBP) and undifferentiated NSCs/NPCs (Nestin) among GFP-positive cells were similar between control and MeCP2-expressing virus-infected cells (Figs. 1B, C and Supplemental Fig 1B). When we extended the culture period after virus infection to 8 days, the percentage of Nestin-positive cells among GFP-positive cells decreased to 10–20% in both control and

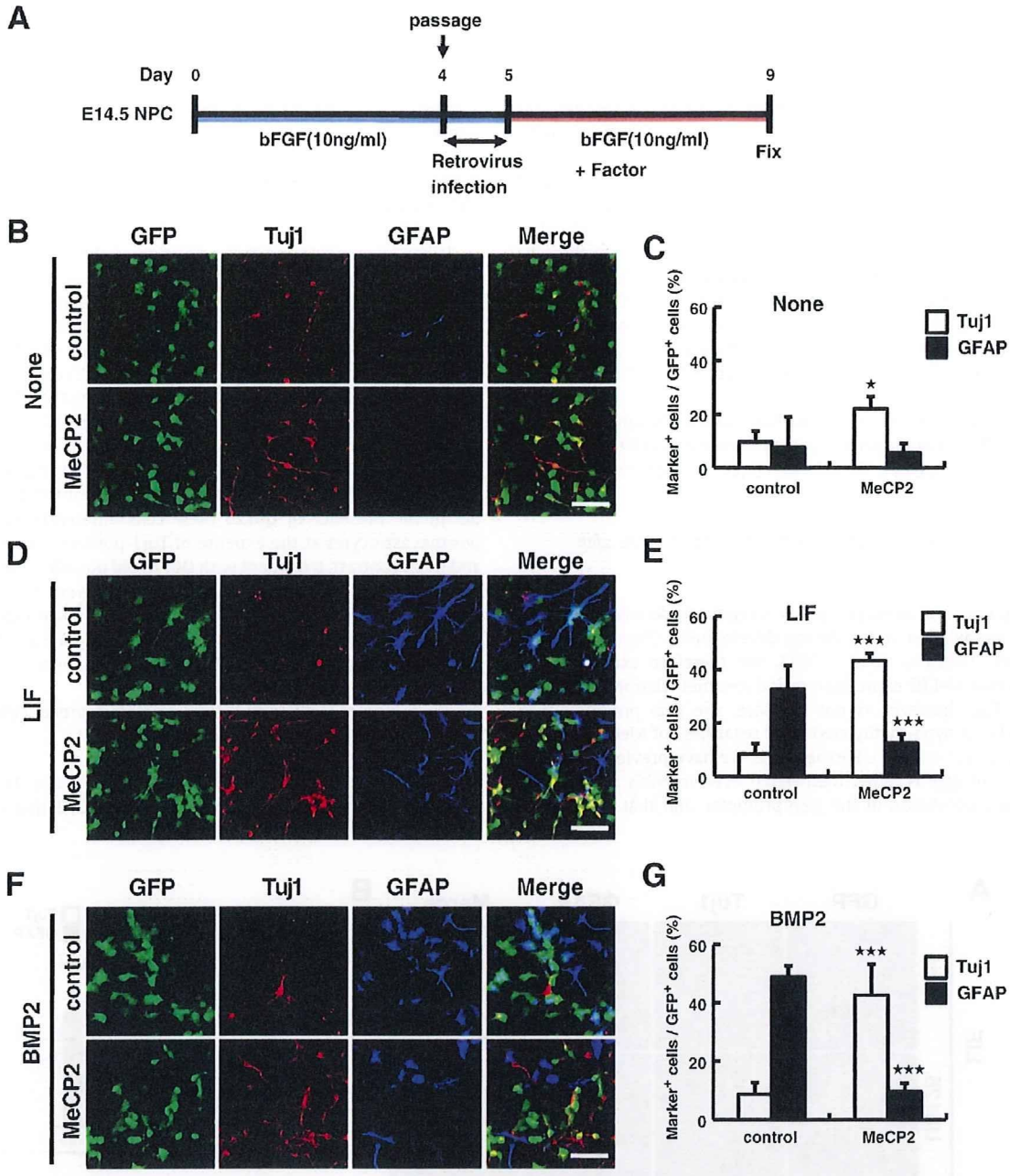

Fig. 1. MeCP2 promotes neurogenesis even in the presence of astrocyte-inducing cytokines. (A) Schematic of the cell culture and virus infection time course. (B, D and F) NPCs infected with recombinant retroviruses engineered to express only GFP (upper panels) or MeCP2 together with GFP (lower panels) were cultured for 4 days in the presence of bFGF (1 ng/ml) alone (B) or together with either LIF (50 ng/ml) (D) or BMP2 (50 ng/ml) (F). The cells were then stained with antibody for GFP (green), βIII-tubulin (Tuj1, red) and GFAP (blue). Scale bar = 50 μm. (C, E and G) Tuj1- and GFAP-positive cells in GFP-positive cells in (B), (D) and (F) were quantified (mean ± S.D.; *t*-test, $*P<0.05$ and $***P<0.001$ compared with the control).

MeCP2-expressing cells, suggesting that the NPC population had matured compared to the 4-day culture (Supplemental Fig. 1C). Even in this prolonged culture, MeCP2 expression still promoted neuronal differentiation of NPCs compared to control (Supplemental Fig. 1C).

To examine whether MeCP2 can induce neuronal differentiation even in the presence of astrocyte-inducing factors, virus-infected NPCs were cultured with LIF or BMP2. As we have shown previously, MeCP2 expression inhibited cytokine-induced astrocytic differentiation of NPCs. Surprisingly, MeCP2 could promote neuronal differentiation more effectively in the presence of LIF than in its absence (Figs. 1D and E). This effect of MeCP2 was also observed with BMP2 (Figs. 1F and G). Moreover, MeCP2 enhanced expression of another neuronal marker, MAP2ab, in the presence of either LIF or BMP2 (Supplemental Figs. 2A and B). We further examined whether MeCP2 suppresses other astrocytic markers in the presence of LIF, and found that MeCP2 indeed inhibited the expression of AQP4 and S100β (Supplemental Fig. 3).

We then asked whether this fate switch was due to increased proliferation and/or survival of NPCs expressing MeCP2. E14.5 NPCs were infected with retrovirus to express GFP either alone or together with MeCP2. Two days later, we assessed cell proliferation and survival by immunocytochemistry using antibodies against Ki-67 (a

proliferation marker) or cleaved-caspase3 (an apoptosis marker) (Supplemental Fig. 4). The expression of MeCP2 had no significant effect on either proliferation or apoptosis (Supplemental Figs. 4B and C).

Since NPCs in primary culture are known to be a heterogeneous population containing differentiated neural cells as well as multipotent and lineage-committed NPCs, we performed the same experiments as those in Fig. 1 using NSCs, which had been cultured under conditions that sustain pure symmetrical divisions of NSCs without accompanying differentiation (Conti et al., 2005; Pollard et al., 2006). As shown in Supplemental Fig. 5A, almost all of the cells were immunoreactive for the undifferentiated NSC/NPC markers Sox2 and Nestin; none was stained by antibodies for the differentiation markers Tuj1, GFAP and MBP. Even in this homogeneous population, MeCP2 expression enhanced neuronal differentiation to an extent comparable to that observed in the primary NPC culture (Supplemental Figs. 5B–F).

Collectively, these results indicate that MeCP2 not only suppresses astrocytic differentiation but also promotes neuronal differentiation of multipotent NSCs/NPCs in the presence of astrocyte-inducing cytokines.

MeCP2 expression does not affect methylation status of the gfap promoter

The expression of astrocytic genes is regulated decisively by their promoter methylation status during development (Namihira et al., 2004, 2009; Takizawa et al., 2001). We therefore examined the possibility that MeCP2 expression re-induces methylation in the *gfap* promoter. This, however, is not the case: the *gfap* promoter was maintained in a hypo-methylated state regardless of MeCP2 expression (Supplemental Fig. 6). Furthermore, we have previously shown that exon 1 of *gfap* is hyper-methylated even in NPCs which have already lost methylation in the *gfap* promoter, and that MeCP2 can bind to the hyper-methylated exon 1 to suppress *gfap* expression (Setoguchi et al., 2006; Kohyama et al., 2008). Sustained hyper-methylation of the *gfap* exon 1 in control and MeCP2-expressing virus-infected cells was also confirmed in the present study, suggesting that MeCP2 binds this region to inhibit astrocytic gene expression.

Inhibition of the Ras-ERK pathway abolishes MeCP2-mediated neuronal differentiation

It has been suggested that activation of the Ras-ERK pathway is important for neuronal differentiation (Menard et al., 2002; Paquin et al., 2005). The culture medium used in our experiments contains insulin and bFGF, which activate the Ras-ERK pathway (Avruch, 1998; Kouhara et al., 1997). Therefore, we examined whether the anti-gliogenic and pro-neurogenic functions of MeCP2 require activation of the Ras-ERK pathway, using U0126, an inhibitor of the ERK-upstream kinase MEK. NPCs were infected with control and MeCP2-expressing retroviruses and cultured with or without U0126 in the presence of bFGF (1 ng/ml) and LIF (50 ng/ml). MeCP2-expressing NPCs differentiated into Tuj1-positive neurons without U0126 as in Fig. 1, but in the presence of U0126 these cells differentiated into GFAP-positive astrocytes at the expense of Tuj1-positive neurons (Figs. 2A and B). In contrast, treatment with U0126 did not affect differentiation of control virus-infected NPCs. Similar results were also obtained in the case of BMP2 stimulation (Figs. 2A and C). Taken together, these observations suggest that the Ras-ERK pathway plays a critical role in MeCP2-mediated regulation of NPC fate specification.

A mutant form of MeCP2 can neither promote neuronal differentiation nor suppress astrocytic differentiation

Mutations in *mecp2* cause RTT (Amir et al., 1999). To determine whether a representative mutant form of MeCP2 that is found in

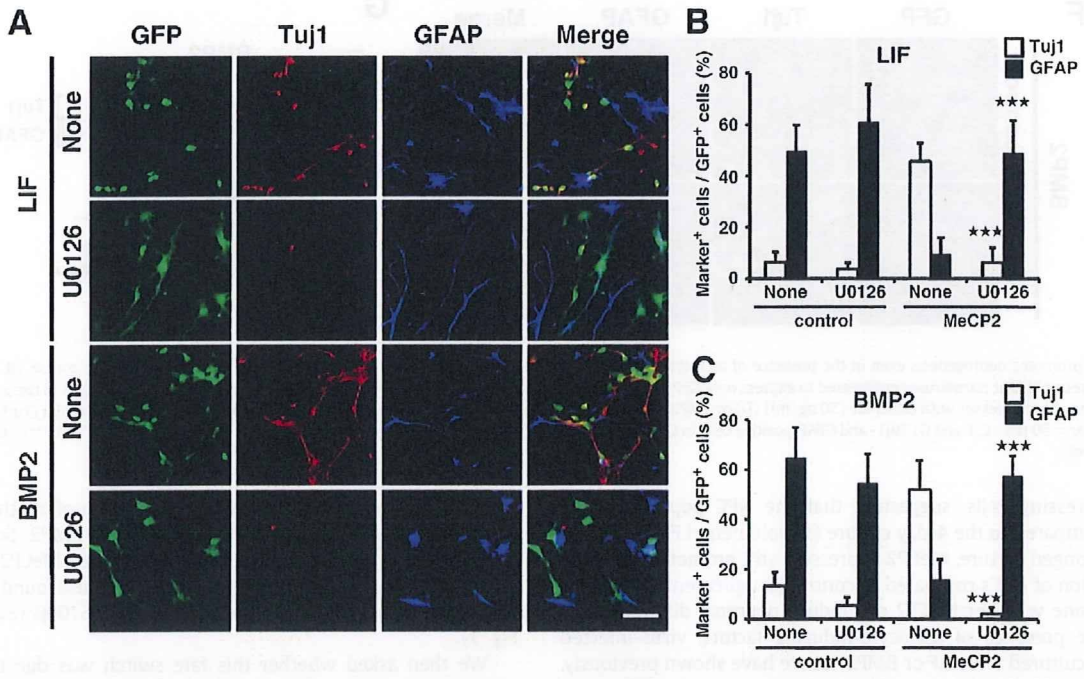

Fig. 2. Inhibition of the Ras-ERK pathway abolishes neuronal differentiation mediated by MeCP2. (A) NPCs infected with recombinant retroviruses engineered to express only GFP (not shown) or MeCP2 together with GFP were cultured with (second and bottom rows) or without (top and third rows) the MEK inhibitor U0126 (8 μM) for 4 days in the presence of bFGF (1 ng/ml) together with either LIF (50 ng/ml) or BMP2 (50 ng/ml). The cells were then stained with antibody for GFP (green), βIII-tubulin (Tuj1, red) and GFAP (blue). Scale bar = 50 μm. (B and C) Tuj1- and GFAP-positive cells in GFP-positive cells cultured as in (A) were quantified (mean ± S.D.; *t*-test, ***$P<0.001$ compared with the control).

RTT patients also exerts the dual function of wild type MeCP2 described above, i.e., inhibition of glial differentiation and promotion of neuronal differentiation, we used R168X, a truncated mutant form of MeCP2 which is observed at high frequency in classic RTT (Amir and Zoghbi, 2000) and lacks the C-terminal two-thirds of the polypeptide including the TRD (Fig. 3A). NPCs were infected with full-length MeCP2- or R168X-expressing retroviruses and cultured in the presence of LIF for 4 days. In contrast to the behavior of intact MeCP2, R168X was unable either to enhance neuronal differentiation or to suppress astrocytic differentiation (Figs. 3B and C). This loss of wild type MeCP2 function was also displayed by R168X in the presence of BMP2 (Figs. 3D and E). These results indicate that the TRD and C-terminal region are required for the dual function of MeCP2.

MeCP2 enhances neuronal differentiation of NPCs in non-neurogenic regions in vivo

BMP2 and/or BMP4 are physiologically expressed in the striatum, a non-neurogenic region in the adult brain, where they inhibit neurogenesis (Gross et al., 1996; Lim et al., 2000). Given that MeCP2 promotes neuronal differentiation even in the presence of BMP2 in *in vitro* experiments, we next asked whether MeCP2 can also enhance neuronal differentiation and suppress astrocytic differentiation in the striatum. We transplanted NPCs infected with retroviruses expressing GFP (control) or GFP together with MeCP2 into the striatum (Fig. 4A). One week after transplantation, more than half of the control NPCs had differentiated into GFAP-positive astrocytes (Figs. 4B and C). In marked contrast, NPCs expressing MeCP2 differentiated dramatically into DCX-positive immature neurons. Quantitative analysis revealed that 59% and only 11% of control NPCs became GFAP- and DCX-immunoreactive cells, respectively, whereas 10% and 62% of MeCP2-expressing NPCs became GFAP- and DCX-immunoreactive cells, respectively (Fig. 4C). This differentiation tendency was also observed at 2 weeks post-transplantation (Supplemental Fig. 7A). Thus, these results reveal that MeCP2 enhances neuronal differentiation and inhibits astrocytic differentiation in the striatum, a well-known non-neurogenic region.

A previous study has suggested that NPCs grafted into another non-neurogenic region, the spinal cord, were restricted to the glial

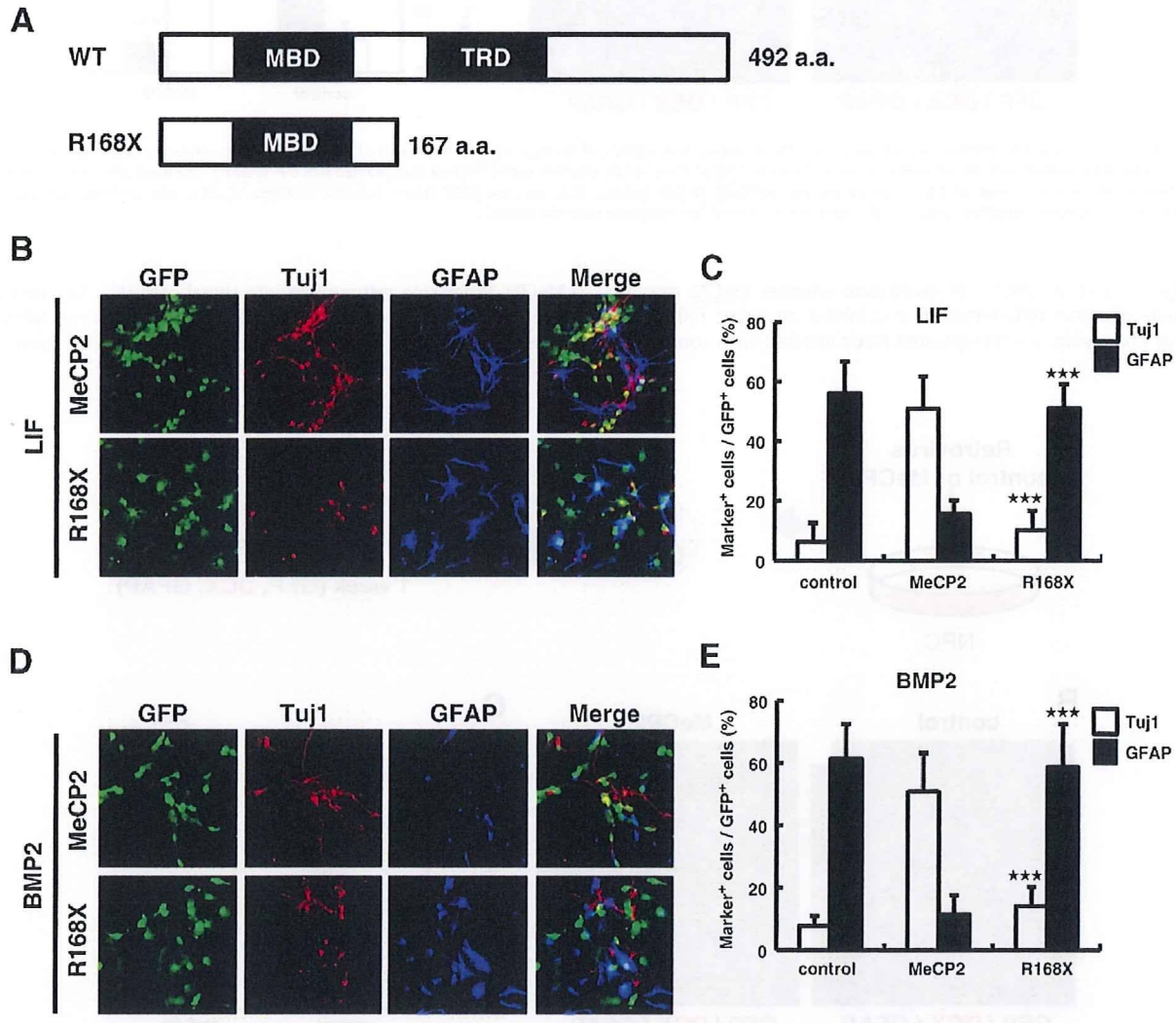

Fig. 3. A truncated form of MeCP2 found in RTT patients cannot promote neuronal differentiation. (A) Schematic illustration of full-length (WT) and a mutant form (R168X) of MeCP2. a.a., amino acids. (B and D) NPCs infected with recombinant retroviruses engineered to express MeCP2 together with GFP or R168X together with GFP were cultured for 4 days in the presence of bFGF (1 ng/ml) together with either LIF (50 ng/ml) (B) or BMP2 (50 ng/ml) (D). The cells were then stained with antibody for GFP (green), βIII-tubulin (Tuj1, red) and GFAP (blue). Scale bar = 50 μm. (C and E) Tuj1- and GFAP-positive cells in GFP-positive cells in (B) and (D) were quantified (mean ± S.D.; *t*-test, ***$P<0.001$ compared with WT MeCP2).

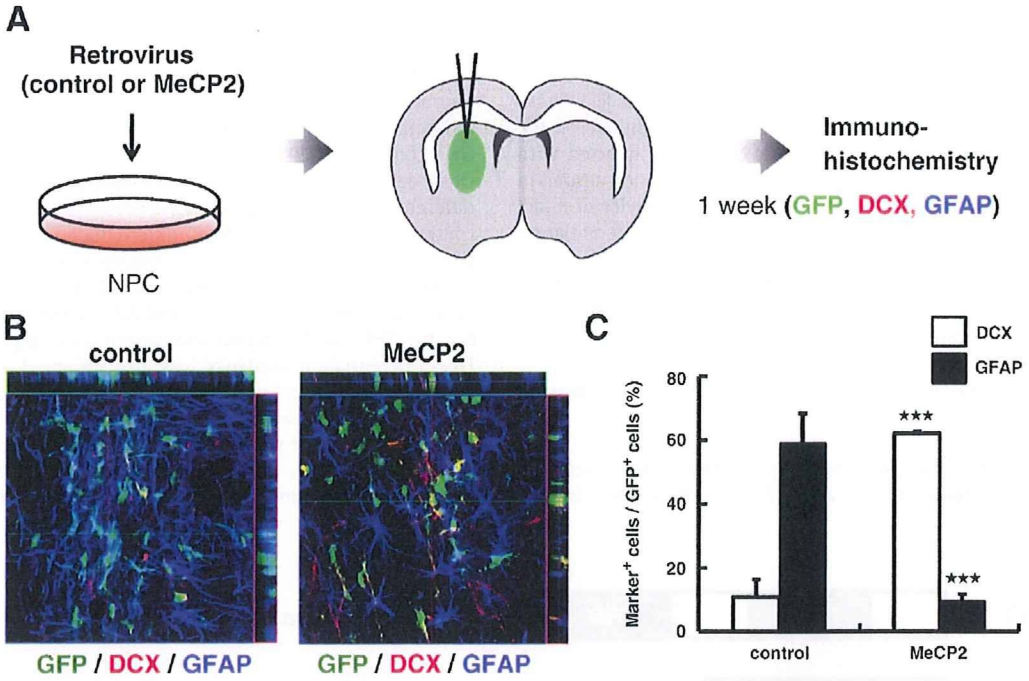

Fig. 4. MeCP2-expressing NPCs differentiate into neurons in the striatum. (A) Schematic of the experiment. The green oval indicates the cell-transplanted region in the striatum. (B) NPCs infected with recombinant retroviruses engineered to express only GFP or MeCP2 together with GFP were transplanted into the striatum. One week after transplantation, the mice were killed and brain tissue sections were stained with antibody for GFP (green), DCX (red) and GFAP (blue). Scale bar = 50 μm. (C) DCX- and GFAP-positive cells in GFP-positive cells in (B) were quantified (mean ± S.D.; *t*-test, $n = 3$; ***$P < 0.001$ compared with the control).

lineage (Cao et al., 2001). To investigate whether MeCP2 can also promote neuronal differentiation and inhibit astrocytic differentiation in this region, we transplanted NPCs infected with control and MeCP2-expressing retroviruses into spinal cord (Fig. 5A). One week after transplantation, we found that 56% of control NPCs had differentiated into GFAP-positive astrocytes and 9% into DCX-

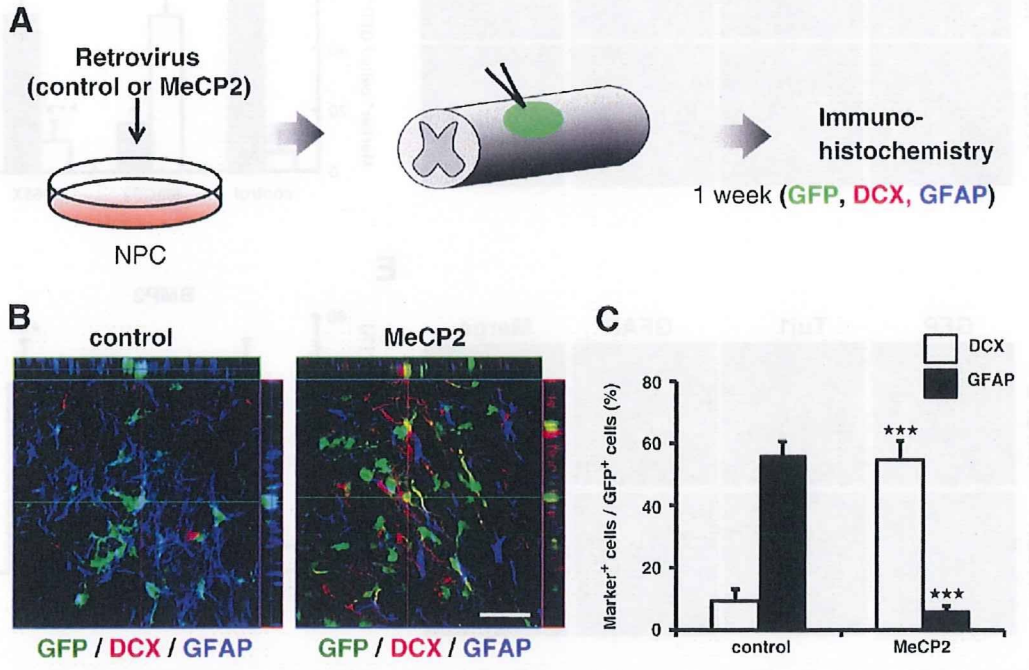

Fig. 5. MeCP2-expressing NPCs differentiate into neurons in the spinal cord. (A) Schematic of the experiment. The green oval indicates the cell-transplanted region in the spinal cord. (B) NPCs infected with recombinant retroviruses engineered to express only GFP or MeCP2 together with GFP were transplanted into the intact spinal cord. One week post-transplantation, the mice were killed and spinal cord tissue sections were stained with antibody for GFP (green), DCX (red) and GFAP (blue). Scale bar = 50 μm. (C) DCX- and GFAP-positive cells in GFP-positive cells in (B) were quantified (mean ± S.D.; *t*-test, $n = 3$; ***$P < 0.001$ compared with the control).

positive neurons. In contrast to the control NPCs, 54% of transplanted MeCP2-expressing NPCs differentiated into DCX-positive neurons and 6% into GFAP-positive astrocytes (Figs. 5B and C). These tendencies were also observed at 2 weeks post-transplantation (Supplemental Fig. 7B). MeCP2 therefore also enhances neuronal differentiation and inhibits astrocytic differentiation of NPCs in the non-neurogenic spinal cord.

Discussion

Mutations in *mecp2* cause Rett syndrome. MeCP2 is expressed predominantly in neurons in the CNS and functions as a repressor of gene transcription. However, the molecular mechanisms by which MeCP2 dysfunction leads to the neural-specific phenotypes of RTT remain poorly understood (Chen et al., 2001). Kishi and Macklis (2004) have reported that MeCP2 is involved in neuronal maturation rather than cell fate determination, as judged from both *in vivo* and *in vitro* analysis of MeCP2 mutant mice. In the present study, we have demonstrated that ectopic expression of MeCP2 in NPCs not only suppresses astrocytic differentiation but also promotes neuronal differentiation in both *in vitro* and *in vivo* conditions. These results clearly suggest that MeCP2 has the potential to regulate fate determination of NPCs under certain circumstances. We also showed that R168X, a truncated form of MeCP2 found in RTT patients, lacks the dual function of full-length MeCP2. This finding indicates that R168X is not functional and may partially explain RTT pathology. In support of this, it has been reported that transcription of several astrocytic genes, including *gfap*, is upregulated in RTT patients (Colantuoni et al., 2001).

The Ras-ERK pathway has been suggested to be important for neuronal differentiation of NPCs (Menard et al., 2002; Paquin et al., 2005). We demonstrated in this study that the MEK inhibitor U0126 abolished the capacity of MeCP2 to promote neuronal differentiation and to suppress astrocytic differentiation, suggesting that ERK activation is, at least in part, involved in the function of MeCP2. Thus, it is possible that MeCP2 is phosphorylated by ERK to form a functional complex with other relevant proteins. Regarding MeCP2 phosphorylation, it has been reported that MeCP2 is phosphorylated at serine 421 by a CaMKII-dependent mechanism in response to neuronal activity, and is also phosphorylated at serines 80 and 229 independently of neuronal activity (Zhou et al., 2006). In this context, we constructed three mutant forms of *mecp2*, each encoding a single serine-to-alanine mutation at position 80, 229 or 421. However, these mutants exerted the same dual function as was observed with intact MeCP2 (data not shown).

An important question still remains unsolved: how does MeCP2 respectively enhance and inhibit neuronal and astrocytic differentiation? One possibility is that MeCP2 represses the expression of repressors of neuronal differentiation such as neuron-restrictive silencer factor/RE-1 silencing transcription factor (NRSF/REST), which is a repressor of neuronal genes in non-neuronal cells (Chong et al., 1995; Schoenherr and Anderson, 1995). It has been suggested that neurogenin1 (NEUROG1), a proneural basic helix–loop–helix (bHLH) transcription factor, can inhibit transcription of *gfap* by sequestering the CREB binding protein (CBP)-Smad1 complex away from astrocyte-specific genes and by inhibiting the activation of STATs, which are necessary for astrocyte differentiation (Sun et al., 2001). Therefore, it is possible that expression of proneural bHLH genes such as *Neurog1* is somewhat induced, and that the gene product(s) function in concert with MeCP2. It has recently been suggested that MeCP2 associates with the transcriptional activator cAMP responsive element binding protein (CREB) and can thereby function as an activator of transcription (Chahrour et al., 2008). CREB was shown to be phosphorylated by ERK (Brami-Cherrier et al., 2005). Thus, it is likely that MeCP2 associates with phosphorylated CREB to function as a transcriptional activator, which may explain why the MEK inhibitor U0126 impeded MeCP2-mediated neuronal differentiation of NPCs. However, further investigation will be needed to precisely verify the mechanism whereby MeCP2 regulates differentiation of NPCs.

Since spontaneous recovery is very limited in the damaged mammalian CNS, NPCs are currently considered a promising cell source for cell replacement strategies aimed at treating neurodegenerative diseases and CNS injuries. Inflammatory cytokines, such as LIF and BMPs, which promote astrocytic differentiation are upregulated in lesion sites of the CNS (Nakamura et al., 2003; Setoguchi et al., 2004). Adult NPCs proliferate in response to injury, but the vast majority of newly generated cells differentiate into astrocytes (Johansson et al., 1999; Namiki and Tator, 1999), and this is also the case for exogenous NPCs that are transplanted into the injured CNS (Ogawa et al., 2002; Vroemen et al., 2003). This astrocytic differentiation of NPCs at the expense of neuronal differentiation is one of the major current obstacles in regeneration therapy. The gliogenic environment pertaining in the adult CNS is thought to be governed by extrinsic environmental factors, such as LIF and BMPs. Thus, tools that are capable of preventing astrocytic differentiation and stimulating other lineages in endogenous NSCs and grafted cells may be key factors for functional recovery. In this study, we have demonstrated that MeCP2 dramatically enhances neuronal differentiation and inhibits astrocytic differentiation even in the presence of astrocyte-inducing cytokines, both *in vitro* and in non-neurogenic striatum and spinal cord *in vivo*, raising the possibility that MeCP2 could be used to regulate NPC fate decision and thereby to improve functional recovery in the damaged CNS.

A previous study suggested that transduction of NPCs with *Neurog2* before transplantation inhibited astrocyte differentiation and improved functional recovery in the rat model of spinal cord injury (Hofstetter et al., 2005). However, the expression of *Neurog2* is transient during development, and is downregulated when neurons become mature. Therefore, continuous expression of *Neurog2* in engrafted cells might lead to unforeseen adverse side-effects. On the other hand, MeCP2 protein levels increase as neurons mature, and *mecp2* expression is sustained in mature neurons (Kishi and Macklis, 2004). We therefore anticipate that transduction of NPCs with *mecp2* would have fewer undesirable side-effects than that with *Neurog2*. However, it has also been reported that expression levels of MeCP2 are critical for normal neurological function (Chao et al., 2007), and that transgenic mice expressing excess *mecp2* display neurological dysfunction similar to that seen in RTT (Collins et al., 2004). To achieve optimal regulation of neuronal function, therefore, it may be necessary to control the MeCP2 expression level in NPCs.

In conclusion, our findings open a promising new avenue for promoting the ability of NPCs to generate the large numbers of neurons that will be required for restorative treatment of neurodegenerative disorders and injured nervous systems. Testing this possibility must await further investigation.

Acknowledgments

We thank Dr. T. Kitamura (Tokyo University) for pMY vector and Plat-E cells. We appreciate Drs. Y. Bessho and T. Matsui for valuable discussions. We also thank Dr. I. Smith for helpful comments and critical reading of the manuscript. We are very grateful to N. Ueda and M. Tano for excellent secretarial assistance. Many thanks to N. Namihira for technical help. This work has been supported by the Suzuken Memorial Foundation, the TERUMO Lifescience Foundation, the Mochida Memorial Foundation for Medical and Pharmaceutical Research, and by a Grant-in-Aid for Science Research on Priority Areas and the NAIST Global COE Program (Frontier biosciences: strategies for survival and adaptation in a changing global environment) from the Ministry of Education, Culture, Sports, Science and Technology of Japan.